© 2014. Published by The Company of Biologists Ltd | Journal of Cell Science (2014) 127, 4064–4077 doi:10.1242/jcs.153346

RESEARCH ARTICLE

Divergent and convergent roles for kinases and phosphatases in neurofilament dynamics

Sangmook Lee[1,*], Harish C. Pant[2,*] and Thomas B. Shea[1,*]

ABSTRACT

C-terminal neurofilament phosphorylation mediates cation-dependent self-association leading to neurofilament incorporation into the stationary axonal cytoskeleton. Multiple kinases phosphorylate the C-terminal domains of the heavy neurofilament subunit (NF-H), including cyclin-dependent protein kinase 5 (CDK5), mitogen-activated protein kinases (MAPKs), casein kinase 1 and 2 (CK1 and CK2) and glycogen synthase kinase 3β (GSK3β). The respective contributions of these kinases have been confounded because they phosphorylate multiple substrates in addition to neurofilaments and display extensive interaction. Herein, differentiated NB2a/d1 cells were transfected with constructs expressing GFP-tagged NF-H, isolated NF-H sidearms and NF-H lacking the distal-most 187 amino acids. Cultures were treated with roscovitine, PD98059, Li^+, D4476, tetrabromobenzotriazole and calyculin, which are active against CDK5, MKK1 (also known as MAP2K1), GSK3β, CK1, CK2 and protein phosphatase 1 (PP1), respectively. Sequential phosphorylation by CDK5 and GSK3β mediated the neurofilament–neurofilament associations. The MAPK pathway (i.e. MKK1 to ERK1/2) was found to downregulate GSK3β, and CK1 activated PP1, both of which promoted axonal transport and restricted neurofilament–neurofilament associations to axonal neurites. The MAPK pathway and CDK5, but not CK1 and GSK3β, inhibited neurofilament proteolysis. These findings indicate that phosphorylation of neurofilaments by the proline-directed MAPK pathway and CDK5 counterbalance the impact of phosphorylation of neurofilaments by the non-proline-directed CK1 and GSK3β.

KEY WORDS: Neurofilament, Kinase, Phosphatase, Axonal stability, Cytoskeleton

INTRODUCTION

Mammalian neurofilaments consist of three subunits, termed NF-H, NF-M and NF-L (corresponding to heavy, medium and light, according to their molecular mass) (Nixon and Shea, 1992; Pant and Veeranna, 1995), along with α-internexin and peripherin (Yuan et al., 2006; Yuan et al., 2012). NF-H and NF-M C-terminal phosphorylation fosters divalent-cation-dependent neurofilament–neurofilament interactions that mediate the formation of the stationary cytoskeleton, which provides support to the axon (Nixon, 1998; Yabe et al., 2001b; Shea and Lee, 2011; Shea and Lee, 2013). Extensively phosphorylated neurofilaments are normally segregated within axons through a complex interaction of kinases and phosphatases, disruption of which fosters aberrant accumulation of neurofilament spheroids within perikarya and proximal axons resembling those that occur during amyotrophic lateral sclerosis (ALS) (Pant and Veeranna, 1995; Julien and Mushynski, 1998; Sihag et al., 2007).

Kinases regulating neurofilament dynamics include cyclin-dependent protein kinase 5 (CDK5), mitogen-activated protein kinases (MAPKs), casein kinase 1 and 2 (CK1 and CK2), glycogen synthase kinase 3α and 3β (GSK3α and GSK3β), p38 MAPK and c-Jun terminal kinase (JNK) (Guan et al., 1991; Link et al., 1992; Guidato et al., 1996; Bajaj and Miller, 1997; Giasson and Mushynski, 1997; Veeranna et al., 1998; Bajaj et al., 1999; Li et al., 1999; Ackerley et al., 2000; Ackerley et al., 2003; Kesavapany et al., 2003; Waetzig and Herdegen, 2003; Chan et al., 2004; Barry et al., 2007; DeFuria and Shea, 2007; Perrot et al., 2008; Holmgren et al., 2012). Phosphatases that regulate neurofilament dynamics include protein phosphatase 1, 2A and 2B (PP1, PP2A and PP2B) (Shea et al., 1993; Saito et al., 1995; Strack et al., 1997; Jung and Shea, 1999; Gong et al., 2003; Veeranna et al., 2011).

Elucidation of the respective contribution of these kinases has been confounded because they mediate multiple integral roles in neuronal homeostasis (Maccioni et al., 2001; Galletti et al., 2009; Pucilowska et al., 2012; Shukla et al., 2012; Pan et al., 2013), are activated independently of neurofilament dynamics and display considerable crosstalk. For example, the MAPK pathway (i.e. MKK1 to ERK1/2) downregulates GSK3β (Ding et al., 2005). GSK3β activates MAPK pathway activity, whereas CDK5 inhibits the MAPK pathway (Noh et al., 2012) (Zheng et al., 2007). CK1-mediated phosphorylation primes several GSK3β substrates (Hagen et al., 2002; Harwood, 2002; Wang et al., 2002; Hergovich et al., 2006) and regulates CDK5 activity (Liu et al., 2001). Finally, the phosphatases that dephosphorylate neurofilaments can also positively and negatively regulate neurofilament kinases (Goldberg, 1999; Adams et al., 2005).

To surmount these difficulties, we utilized NB2a/d1 cells, which express and phosphorylate all neurofilament subunits and establish a stationary phase within axonal neurites. These cells are readily transfected, allowing selective manipulation of kinases and phosphatases, and can be grown in bulk to allow a combination of immunofluorescence analyses and immunological analyses of cellular fractions. This reductionist approach elucidated divergent and convergent roles for CK1, GSK3β, the MAPK pathway, CDK5 and PP1 in neurofilament dynamics.

RESULTS

Neurofilaments containing extensively phosphorylated NF-H are expressed by and incorporated into the cytoskeleton of

[1]Center for Cellular Neurobiology and Neurodegeneration Research, Department of Biological Sciences, University of Massachusetts Lowell, Lowell, MA 01854, USA. [2]Cytoskeletal Protein Regulation Section, NIH, NINDS, Bethesda, MD 20892, USA.

*Authors for correspondence (sangmook_lee@uml.edu; PantH@ninds.nih.gov; thomas_shea@uml.edu)

Received 17 March 2014; Accepted 1 July 2014

Journal of Cell Science

Journal of Cell Science (2014) 127, 4064–4077 doi:10.1242/jcs.153346

differentiated NB2a/d1 cells (Fig. 1A,B). In efforts to identify which kinase(s) were predominantly responsible for generation of commonly studied neurofilament phospho-epitopes, we overexpressed the known neurofilament kinases CDK5, MAPK, GSK3β and CK1. Increased activity of CDK5 and the MAPK pathway have previously been demonstrated within these cells following transfection with p25 (a positive regulator of CDK5) and constitutively active MKK1 (Chan et al., 2004; Shea et al., 2004). We confirmed increased activity of GSK3β and CK1 following transfection, and their inhibition following Li^+ and D4476 treatment (Fig. 1C,D). Homogenates of cells overexpressing these kinases were subjected to immunoblot analyses. Given that

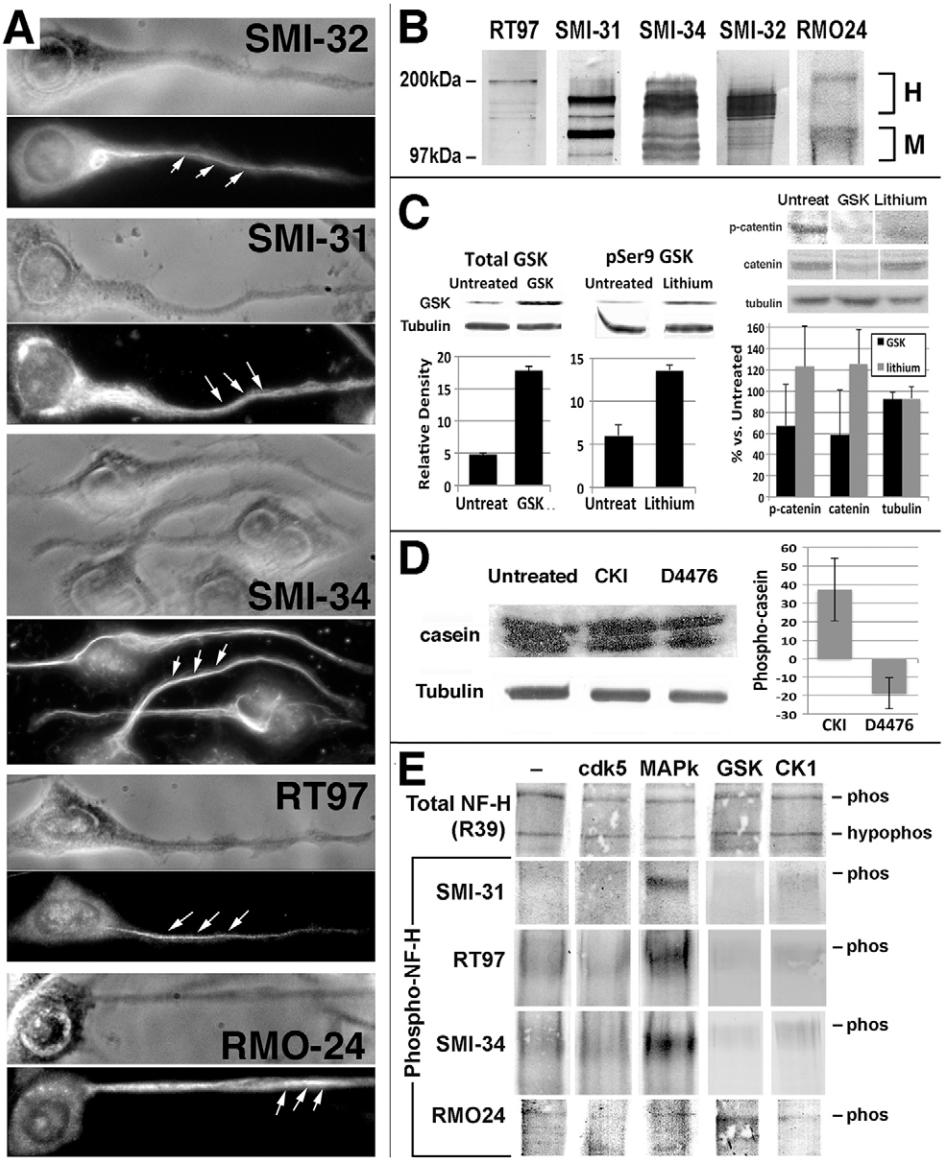

Fig. 1. Neurofilament phospho-epitopes in NB2a/d1 cells and the kinases responsible. (A) Representative differentiated cells probed with antibodies directed against phospho- (RT97, SMI-31, SMI-34, RMO-24) and nonphospho- (SMI-32) epitopes as indicated. Note the centrally situated neurofilament bundle along neurites (arrows). (B) Nitrocelluose replicas of homogenates probed with the above antibodies; migration of NF-H (H) and NF-M (M) are indicated. (C) Transfection with a construct expressing GSK3β (GSK) significantly ($P<0.05$) increased overall GSK3β levels [which increases net GSK3β activity (Wagner et al., 1996)], and decreased levels of the GSK3β substrate β-catentin (pSer9 GSK, which is proteolyzed following GSK3β-mediated phosphorylation). Li^+ significantly increased levels of GSK3β phosphorylated at Ser9 [which inactivates GSK3β (Lamarre and Desrosiers, 2008)] and prevented degradation of phospho- and total β-catentin (labeled p-catenin and catenin, respectively). β-tubulin (probed with antibody DM1A) was included as a loading control. The accompanying graphs present the mean±s.e.m. for three immunoblots for total and phospho-GSK3β and two for phospho- and total β-catentin. (D) CK1 overexpression increased, whereas the CK1 inhibitor D4476 decreased, casein phosphorylation versus untreated controls. A representative gel zymograph is presented along with a nitrocellulose replica of an aliquot of the same sample probed with anti-tubulin antibody DM1A as a loading control. The accompanying graph presents the mean±s.e.m. of casein phosphorylation versus untreated controls for three such gels. (E) Nitrocellulose replicas of homogenates overexpressing the indicated kinases (MAPk, MKK1; GSK, GSK3β), probed with the above neurofilament antibodies and a polyclonal antibody (R39) that reacts with neurofilaments regardless of phosphorylation state, as a loading control. Note overexpression of MKK1 increased SMI-31, SMI-34 and RT97 immunoreactivity, whereas GSK3β increased RMO-24. All samples probed with the same antibody in each panel are from the same gel. phos, phosphorylated; hypophos, hypophosphorylated.

Journal of Cell Science (2014) 127, 4064–4077 doi:10.1242/jcs.153346

NB2a/d1 cells contain high levels of phospho- and nonphospho-neurofilaments (Fig. 1B), in order to facilitate detection of any changes in epitopes following selective kinase activation, total aliquots loaded onto gels were restricted, such that the levels in non-transfected cells were barely detectable (Fig. 1E). These analyses indicated that the SMI-31, SMI-34 and RT97 epitopes were predominantly generated by the MAPK pathway. By contrast, the RMO-24 epitope was predominantly generated by GSK3β (Fig. 1E).

To investigate further the potential roles of these kinases on neurofilament phosphorylation, we transfected cells with GFP-tagged neurofilament constructs, which facilitated the monitoring of the levels and distribution of newly expressed neurofilaments independently of differentially phosphorylated endogenous neurofilaments. In addition, expression of GFP-tagged constructs allowed us to more closely monitor the influence of kinase manipulation on neurofilament dynamics without the interference of endogenous neurofilaments.

CK1 mediates the major retardation of NF-H migration on SDS gels

Phosphorylation alters NF-H migration on SDS gels from 160 kDa to 200 kDa (Nixon and Shea, 1992). To determine the responsible kinase(s), we treated cells expressing GFP–NF-H with the above kinase inhibitors plus the casein kinase 2 (CK2) inhibitor tetrabromobenzotriazole (tBBT). The bulk of GFP–NF-H migrated at 195 kDa (Fig. 2), corresponding to hypophosphorylated (160 kDa) NF-H fused to 35-kDa GFP; GFP–NF-H was also detected at 260 kDa (extensively phosphorylated NF-H fused to GFP) (Lee et al., 2011). Phospho-NF-H immunoreactivity was concentrated at the 260-kDa isoform for untreated and Li^+-, PD98059- and roscovitine-treated homogenates. D4476 increased the 195-kDa phospho-NF-H reactivity and reduced the 260-kDa phospho-NF-H reactivity (Fig. 2). D4476 did not alter GFP–NF-H distribution, indicating that this shift in phospho-reactivity was not due to altered migration of total NF-H.

This finding suggests that (1) phosphorylation events mediated by CK1 are crucial for inducing the migratory shift of NF-H to 200 kDa, (2) phosphorylation events mediated by the MAPK pathway, CDK5 and GSK3β are not sufficient to induce this migratory shift, and (3) the SMI-31, SMI-34 and RT97 phospho-epitopes can be generated in the absence of the migratory shift.

CDK5 and GSK3β mediate relatively minor changes in neurofilament migration on SDS gels

The broad band observed for extensively phosphorylated NF-H on SDS gels can be resolved into multiple phospho-dependent isoforms on gels with a low amount of acrylamide (Lewis and Nixon, 1988). GFP–NF-H, and its resultant phospho-isoforms, also appear as a relatively broad band; for example, the phospho-isoform migrating at 260 kDa spans ~10 kDa (e.g. Fig. 3A). To examine further the impact of the above kinases on NF-H migration, we transfected cells with constructs expressing GFP-tagged C-terminal NF-H sidearms, including site-directed mutants in which the Ser residues of CDK5 consensus sequences had been replaced by Asp or Ala residues, termed GFP–NF-Hasp and GFP–NF-Hala sidearms, along with wild-type GFP–NF-H sidearms (i.e. the normal NF-H sidearm) to mimic permanently phosphorylated or nonphosphorylated states (Lee et al., 2011). These site-specific mutations allowed monitoring of potential impact of CDK5 on isoform migration. In addition, these 'tail only' constructs were more sensitive to subtle migratory shifts than were full-length constructs (e.g. Fig. 3B).

SMI-31 and RT97 in wild-type sidearms resolved on low-acrylamide SDS gels into two distinct isoforms migrating at ~200 and 205 kDa. RMO-24 immunoreactivity was exclusively associated with the 205-kDa isoform and a 210-kDa isoform (Fig. 3C). The sidearm construct with Ala substitutions revealed a unique isoform migrating at ~190 kDa, coupled with the loss of the SMI-31- and RT97-reactive 200-kDa isoform (Fig. 3D). RMO-24 immunoreactive isoforms were not affected. This suggests that the migratory shift of this isoform from 190 to

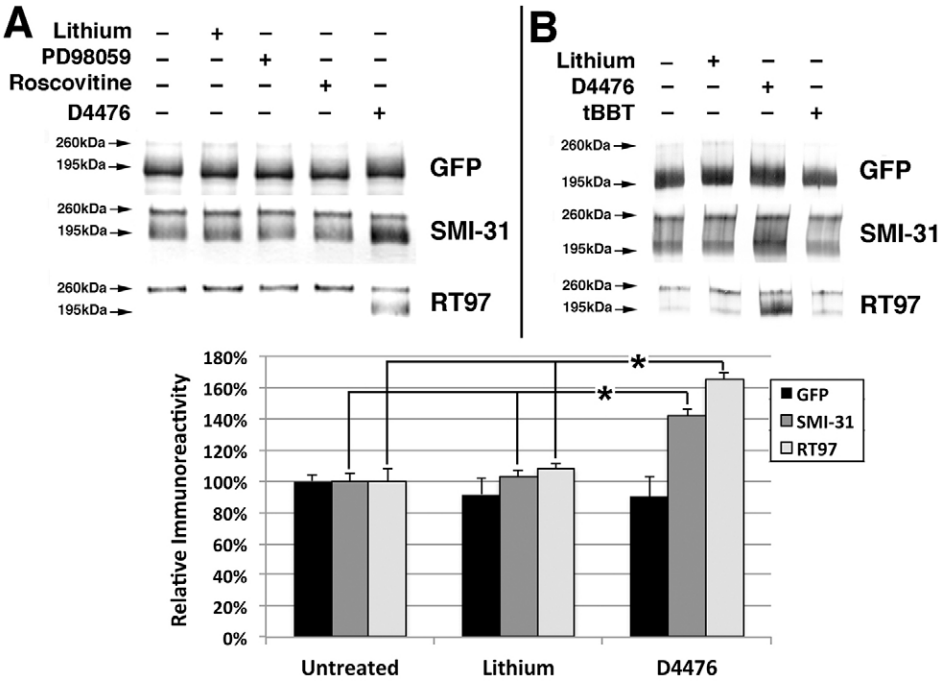

Fig. 2. CK1 mediates the retardation of NF-H migration on SDS gels. (A,B) Nitrocellulose replicas of homogenates transfected 24 h previously with a construct expressing GFP–NF-H and treated for the final 2 h of incubation with the indicated inhibitors, along with homogenates of untreated control cells. The migration of extensively and hypophosphorylated NF-H fused to GFP (260 and 195 kDa) are indicated. Note only D4476 inhibited GFP–NF-H migration. The accompanying graph presents densitometric analyses of 195-kDa NF-H; not all conditions in A and B are included. D4476 treatment did not alter total levels of the 195-kDa isoform, but increased 195-kDa phospho-immunoreactivity versus all other conditions. *$P<0.01$, ANOVA with post-hoc analyses. Values represent the mean±s.e.m. immunoreactivity versus untreated homogenates.

Journal of Cell Science (2014) 127, 4064–4077 doi:10.1242/jcs.153346

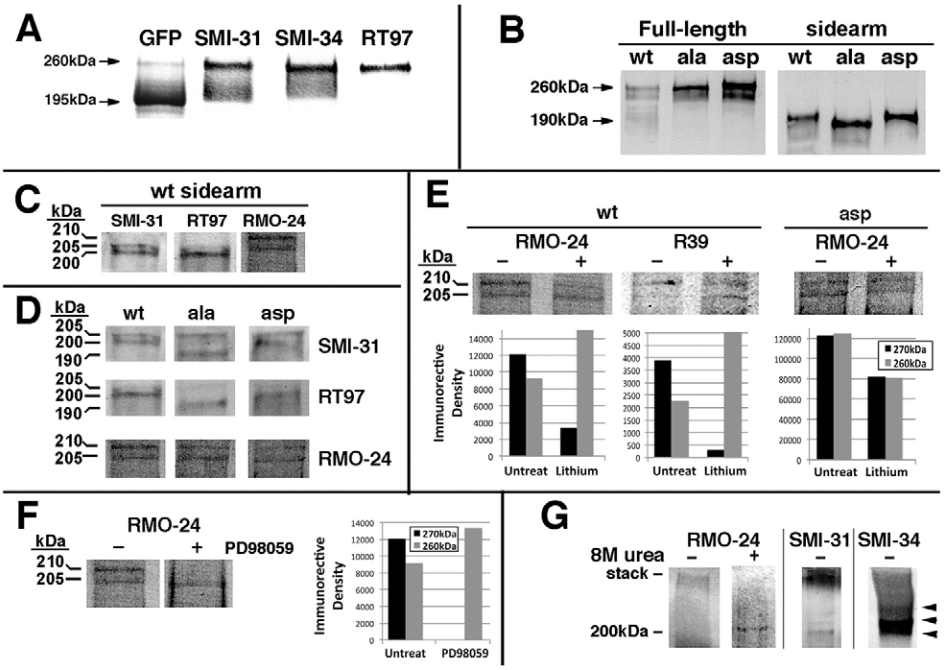

Fig. 3. Multiple kinases generate NF-H isoforms. Nitrocellulose replicas of thin SDS gels of homogenates expressing GFP–NF-H (A,B), GFP-tagged C-terminal sidearms (C–F) or no NF-H construct (G) with or without treatment with Li^+, PD98059 or urea, and probed with anti-GFP, SMI-31, SMI-34, RT97 or R39 (directed against total neurofilaments). (A) GFP–NF-H migrates over a range of 195–260 kDa, which corresponds to the migratory range of NF-H (160–210 kDa) plus the 35-kDa GFP. Phospho-epitopes are concentrated within the slowest-migrating isoforms. (B) Nitrocelluose replicas probed with RT97 of homogenates expressing full-length wild-type (wt) GFP–NF-H, GFP–NF-Hasp or GFP–NF-Hala, or their respective GFP–NF-H sidearm, as indicated. As anticipated, sidearm-only constructs migrate faster on SDS gels. (C) SMI-31 and RT97-reactive isoforms in wild-type GFP–NF-H sidearms resolved on thin SDS gels into isoforms migrating at ~200 and 205 kDa. RMO-24 immunoreactivity was associated with isoforms migrating at 205 and 210 kDa. (D) Nitrocellulose replicas of homogenates expressing wild-type GFP–NF-H, GFP–NF-Hasp or GFP–NF-Hala sidearms probed with the indicated antibodies. Cells expressing the GFP–NF-Hala sidearm lack the 200-kDa isoform but display a 190-kDa isoform that is reactive to SMI-31 and RT97 but not RMO-24. (E) Nitrocellulose replicas of homogenates expressing wild-type GFP–NF-H sidearms or GFP–NF-Hasp sidearms with or without Li^+ treatment probed with RMO-24 or R39. Li^+ depleted the 270-kDa isoform and increased the 205-kDa isoform in wild-type GFP–NF-H sidearms but did not affect the GFP–NF-Hasp sidearm. (F) PD98059 treatment depleted the RMO-24-reactive 210-kDa isoform and increased the 205-kDa isoform. (G) Nitrocellulose replicas of homogenates from non-transfected cells with or without treatment with 8 M urea; the stacking gel was retained for transfer to nitrocellulose as clear NF-H isoforms are only detected following treatment of homogenates with urea prior to electrophoresis. This aggregated material is reactive with SMI-34 and SMI-31; however, clear isoforms from ~210 to 200 kDa (arrows) are detectable in the absence of urea (arrowheads).

200 kDa is mediated by CDK5, given that the Ala substitution specifically blocked CDK5-mediated phosphorylation. Migration of the 205-kDa isoform was not affected, suggesting that its migration was not dependent upon CDK5 activity (Fig. 3D). No difference was detected between migration of GFP–NF-Hasp and wild-type GFP–NF-H sidearms, consistent with the presence of endogenous CDK5 activity in NB2a/d1 cells (Lee et al., 2011; Shea et al., 2004).

The majority of RMO-24 immunoreactivity was derived from GSK3β, because RMO-24 immunoreactivity was reduced by 61%±6 (mean±s.e.m.) following Li^+ treatment; the 210-kDa RMO-24-reactive isoform was more severely depleted, and the 205-kDa isoform was relatively increased (Fig. 3E). This pattern of reduction in isoform reactivity was also observed following probing of additional replicas with a polyclonal antibody (R39) directed against all neurofilaments regardless of phosphorylation state. These findings indicate that GSK3β played a role in shifting the migration of the 205-kDa isoform to 210 kDa. By contrast, the 210-kDa isoform was not depleted in the Asp mutant sidearms (Fig. 3E). Given that Asp mutant sidearms were mutated exclusively at CDK5 consensus sites, this finding indicates that CDK5-mediated phosphorylation plays a role in generation of the 210-kDa isoform in addition to that of GSK3β. PD98059 treatment also depleted the RMO-24-reactive 210-kDa isoform, coupled with an increase in the 205-kDa isoform, suggesting that phosphorylation mediated by the MAPK pathway also contributes to generation of the 210-kDa form.

Although the major shift in migration of NF-H on SDS gels was apparently mediated by CK1 (Fig. 2), these findings demonstrate that generation of the full range of NF-H isoforms involves the MAPK pathway, CDK5 and GSK3β. In contrast to other phospho-dependent neurofilament antibodies, immunoreactivity of NF-H with RMO-24 in non-transfected cells is difficult to detect by immunoblot analyses. However, when the stacking gel was retained for transfer onto nitrocellulose, RMO-24 immunoreactivity was observed within the stack, suggesting that the majority of endogenous RMO-24-reactive NF-H isoforms are associated with SDS-resistant complexes (Fig. 3F). This possibility was confirmed by treatment of cytoskeletal preparations with 8 M urea to dissociate neurofilament complexes (Marston and Hartley, 1990), which eliminated RMO-24 immunoreactivity within the stack and increased immunoreactivity associated with the anticipated migratory position for extensively phosphorylated NF-H. Notably, some SMI-31 and SMI-34 reactivity was observed within this aggregate (Fig. 3G). This is also consistent with detection of the nearly all RMO-24 immunoreactivity within the axonal neurofilament bundle in immunofluorescence analyses (Fig. 1).

Journal of Cell Science (2014) 127, 4064–4077 doi:10.1242/jcs.153346

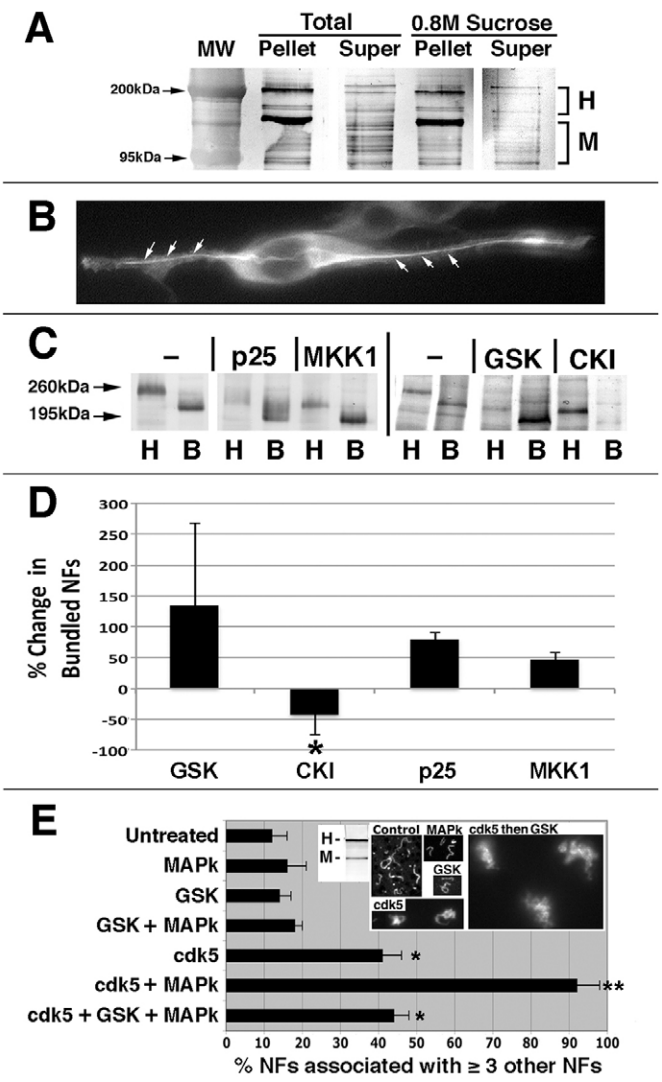

Fig. 4. Kinase activities promote neurofilament bundling. (A) Nitrocellulose replicas of endogenous NF-H (H) and NF-M (M) recovered in total cytoskeletons (Pellet) or remaining in the Triton-soluble supernatant (Super), and neurofilaments that sedimented through a 0.8 M sucrose cushion (Pellet, enriched in bundled neurofilaments) or remaining at the buffer–sucrose interface (Super, enriched in individual, non-bundled neurofilaments) detected with R39. MW, molecular mass markers. (B) A representative epifluorescent image of a cell expressing GFP–NF-H. Note GFP–NF-H distributes throughout cells and is incorporated into the bundle (arrows). (C) Nitrocellulose replicas, probed with anti-GFP, of homogenates (H) and bundle-enriched fractions (B) from cells transfected 24 h previously with GFP–NF-H constructs alone (–) or co-transfected with constructs expressing p25, MKK1, GSK3β (GSK) and CK1. (D) The percentage change in the ratio of bundled:individual neurofilaments in cells transfected with the indicated neurofilament kinase constructs versus those not transfected with kinase constructs; values represent the mean±the range from two independent experiments; incubation with GSK3β, p25 or MKK1 increased neurofilament–neurofilament associations versus untreated neurofilaments ($P<0.05$, ANOVA). CK1 decreased neurofilament associations versus untreated neurofilament and neurofilaments incubated under all other conditions *$P<0.03$; ANOVA with post-hoc analyses. (E) Quantification of Rhodamine-conjugated spinal cord neurofilaments incubated for 2 h with or without the indicated kinases (MAPk, exogenous addition of ERK1/2). Incubation with CDK5 increased neurofilament–neurofilament associations (*$P<0.05$ versus untreated neurofilaments; Student's *t*-test); incubation with CDK5 + GSK3β further increased neurofilament–neurofilament associations (**$P<0.05$ versus CDK5 alone; Student's *t*-test). Incubation with CDK5, GSK3β and MKK1 prevented the GSK3β-mediated increase beyond that observed with CDK5 alone (*$P<0.05$ versus untreated neurofilaments). Insets present a nitrocellulose replica of this preparation probed with SMI-31, depicting NF-H (H) and NF-M (M) phospho-epitopes, and representative epifluorescence images of neurofilaments from these preparations.

Multiple kinases contribute to neurofilament bundling

Axonal neurites contain a centrally situated bundle of closely opposed neurofilaments that undergo transport and turnover more slowly than the surrounding individual neurofilaments (Fig. 1A). Bundled neurofilaments can be separated from surrounding individual neurofilaments by sedimentation over sucrose, indicating that they are physically associated (Kushkuley et al., 2009) (Fig. 4A,B). Neurofilament–neurofilament associations leading to bundling are mediated by cation-dependent cross-bridging of phospho-neurofilaments (Kushkuley et al., 2009; Yabe et al., 2001a). To investigate which kinase(s) mediate the crucial events that promote neurofilament–neurofilament associations, we compared the impact of kinase overexpression or inhibition on intracellular GFP–NF-H distribution, and found that GSK3β activity and, to a lesser extent, CDK5 and MAPK pathway activity increased neurofilament–neurofilament associations, whereas, by contrast, CK1 activity decreased neurofilament–neurofilament associations (Fig. 4C,D).

We also examined the impact of kinase activity in cell-free analyses (Fig. 4E). Individual neurofilaments recovered from spinal cords were conjugated with Rhodamine and incubated with and without purified kinases, after which we quantified the percentage of neurofilaments that were associated with three or more other neurofilaments (Kushkuley et al., 2009). In these cell-free analyses, we were also able to treat isolated neurofilaments with multiple kinases; this was not practical to attempt within intact cells, because it would require transfection with multiple kinase constructs. In cell-free analyses, neither ERK1/2 nor GSK3β promoted neurofilament–neurofilament associations individually or in combination. Consistent with prior studies (Kushkuley et al., 2009), CDK5 induced an ~40% increase in neurofilament–neurofilament associations. By contrast, CDK5 and GSK3β induced neurofilament–neurofilament associations for ~90% of neurofilaments, indicating a synergistic impact of these kinases on neurofilament bundling. Notably, incubation with CDK5, GSK3β and ERK1/2 attenuated the extent of neurofilament–neurofilament associations observed following incubation with CDK5 and GSK3β to the level observed following incubation with CDK5 alone. This is consistent with the possibility that the MAPK pathway interfered specifically with the impact of GSK3β, and not that of CDK5, on neurofilament–neurofilament associations.

Phosphorylation by CDK5 and the MAPK pathway prevent neurofilament proteolysis

C-terminal phosphorylation inhibits neurofilament proteolysis (Grant et al., 2001; Pant and Veeranna, 1995). We therefore compared the relative contribution of the neurofilament kinases to protection against proteolysis. To accomplish this, we treated cells with the pharmacological inhibitors roscovitine, PD98059, Li^+ and D4476, none of which altered GFP–NF-H levels in isolation (Fig. 5A). However, combined treatment with roscovitine and PD98059 significantly reduced total GFP–NF-H and RT97-reactive NF-H levels (Fig. 5A). By contrast, reduction was not observed following treatment with these compounds individually or in combination. Moreover, overexpression of

Journal of Cell Science (2014) 127, 4064–4077 doi:10.1242/jcs.153346

GSK3β or CK1 could not prevent the depletion of GFP–NF-H following combined treatment with roscovitine and PD98059 (Fig. 5B). These findings indicate that phosphorylation events mediated by CDK5 and the MAPK pathway, but not by GSK3β or CK1, protect neurofilaments from proteolysis. Consistent with recent studies (Rao et al., 2012), phospho-neurofilaments within bundles were more resistant to proteolysis than were neurofilaments in homogenates (Fig. 5C). CDK5 and the MAPK pathway might therefore maintain a critical level of neurofilaments, which would indirectly promote neurofilament bundling.

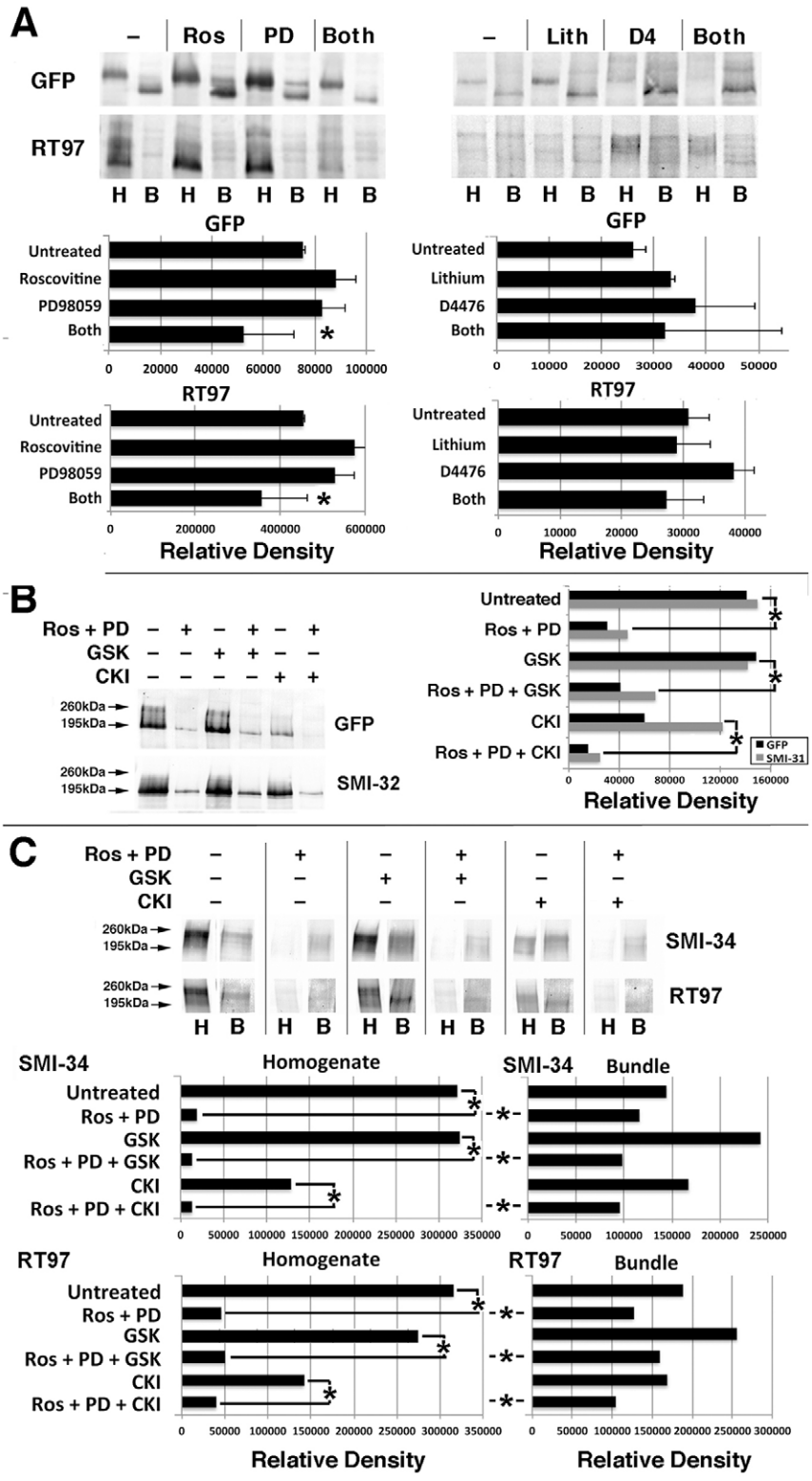

Fig. 5. CDK5 and MAPK protect neurofilaments against proteolysis. (A) Nitrocellulose replicas of homogenates (H) and bundle-enriched fractions (B) from cells treated with roscovitine (Ros), PD98509 (PD) or both, along with untreated controls (Untreat). The accompanying graphs present the total GFP–NF-H (H + B) present under each condition; values represent mean±s.e.m. immunoreactivity from two or three experiments for each condition. Note the specific reduction in GFP–NF-H and RT97 immunoreactivity for cells treated with Ros + PD (*P<0.03, and 0.01 versus all other conditions; ANOVA with post-hoc analyses). (B) Nitrocellulose replicas probed with anti-GFP or non-phospho-specific SMI32 of homogenates (H) from cells treated with Ros+PD with or without overexpression of GSK3β (GSK) or CK1 along with untreated controls. The accompanying graph presents the immunoreactivity present under each condition. Note reduction in levels following treatment with Ros + PD (*P<0.02; ANOVA), and that overexpression of GSK3β or CK1 did not compensate for this treatment (P<0.19 for Ros+PD versus Ros+PD+GSK3β or CK1; ANOVA). (C) Nitrocellulose replicas probed with SMI-34 or RT97 of homogenates (H) and bundle-enriched fractions (B) derived from cells treated as in B. The accompanying graphs present the total immunoreactivity present under each condition. As in B, treatment with Ros+PD reduced phospho-neurofilament immunoreactivity in homogenates in the presence or absence of GSK3β or CK1 (*P<0.01; ANOVA). Note increased depletion in homogenates versus bundles following treatment with Ros+PD with or without overexpression of GSK3β or CK1 (asterisks between graphs, P<0.01; ANOVA).

Journal of Cell Science (2014) 127, 4064–4077 doi:10.1242/jcs.153346

The MAPK pathway mediates anterograde neurofilament transport by inhibiting GSK3β-mediated neurofilament bundling

MAPK pathway activity is required for transport of neurofilaments into and along axons (Chan et al., 2004) but the responsible mechanism remains unclear. Notably, the MAPK pathway inactivates GSK3β (Ding et al., 2005). Herein, we have demonstrated that GSK3β participates in neurofilament bundling, whereas MAPK pathway activity attenuated GSK3β-mediated bundling (Fig. 4). Given that neurofilaments that undergo bundling are withdrawn from the transporting pool (Shea and Lee, 2011), we hypothesized that the mechanism by which the MAPK pathway mediates neurofilament transport might be through inhibiting GSK3β-mediated neurofilament–neurofilament interactions.

If this were indeed the case, we hypothesized that inhibition of neurofilament transport by treatment with PD98059 coupled with overexpression of GSK3β might have an additive effect. To test this possibility, we first confirmed that the MAPK pathway phosphorylated GSK3β at Ser9 (Fig. 6A). Overexpression of GSK3β in which Ser9 was mutated to Ala (GSKala, which cannot be inactivated by phosphorylation and is therefore constitutively active) inhibited neurofilament transport into and along axonal neurites (Fig. 6B). Treatment with PD98059 (which inhibits MAPK pathway activity) inhibits neurofilament transport and fosters perikaryal neurofilament accumulation (Chan et al., 2004) (see also Fig. 6C for representative image). However, when cells overexpressing GSKala were treated with PD98059, we observed an increase in perikaryal neurofilament bundles (Fig. 6C). These findings indicate that the MAPK pathway promotes neurofilament axonal transport by inhibiting GSK3β activity, and in doing so, might preclude inappropriate perkaryal neurofilament bundling.

GSK3β potentiates CDK5-induced neurofilament bundling

Overexpression of CDK5 induces the accumulation of phospho-neurofilament bundles within perikarya (Shea et al., 2004). Given the above demonstration of a crucial role for GSK3β in perikaryal neurofilament accumulation, we questioned whether or not GSK3β participated in CDK5-induced perikaryal neurofilament accumulation. To investigate this possibility, we overexpressed GFP–NF-H along with p25 or GSK3β, and treated cells with Li^+ or roscovitine (inhibitors of GSK3β and CDK5, respectively) prior to harvest. Both p25 and GSK3β overexpression increased the percentage of cells with perikaryal neurofilament bundles. However, treatment with Li^+ inhibited p25-induced perikaryal neurofilament accumulation, and treatment with roscovitine inhibited perikaryal neurofilament accumulation induced by GSK3β (Fig. 6D). These findings indicate that a combination of CDK5 and GSK3β activity is required to induce perikaryal neurofilament accumulations, and are consistent with our demonstration that GSK3β potentiated CDK5-induced neurofilament–neurofilament associations in cell-free analyses (Fig. 4).

CK1 inhibits neurofilament phosphorylation within perikarya by maintaining phosphatase activity

The above results (Fig. 4) indicate that CK1 apparently inhibits neurofilament bundling. This finding seemed counterintuitive, because CK1 activity was responsible for the shift in NF-H migration on SDS gels that was attributed to extensive phosphorylation (Fig. 2), and bundles contain the bulk of extensively phosphorylated neurofilaments (Kushkuley et al., 2009; Yabe et al., 2001a). We therefore examined the levels and distribution of total (GFP–NF-H) and RT97-reactive NF-H within total homogenates and bundle fractions derived from cells following overexpression of CK1 and treatment with D4476 (a pharmacological inhibitor active against CK1) (Fig. 7A). Visual inspection, confirmed by densitometric analyses, revealed that overexpression of CK1 statistically reduced total RT97 immunoreactivity ($P<0.01$, ANOVA), whereas treatment with D4476 statistically increased total RT97 immunoreactivity ($P<0.01$, ANOVA). Overexpression of CK1 decreased the amount of total and RT97-reactive NF-H within bundles (trend towards significance, $P<0.06$, ANOVA), whereas treatment with D4476 increased the amount of total and RT97-reactive NF-H within bundles (trend towards significance, $P<0.08$, ANOVA). Immunofluorescence analyses demonstrated an increase in axonal and perikaryal RT97 reactivity following D4476 treatment (Fig. 7B).

Given that CK1 activates PP1 (Henry and Killilea, 1993), we probed whether or not CK1 regulated neurofilament dynamics through modulation of PP1 activity. D4476 treatment significantly ($P<0.05$) reduced PP1 but not PP2A activity in perikarya and axonal neurites (Fig. 7C). Calyculin, a pharmacological agent active against PP1, fostered the formation of SDS-resistant high-molecular-mass material that was reactive with RT97 but not the nonphospho-neurofilament antibody SMI-32 (Fig. 7D), and increased RT97 immunoreactivity within perikarya and axonal neurites (Fig. 7E). These findings indicate that PP1 activity regulates NF-H C-terminal phosphorylation, including restricting phospho-neurofilament accumulation within perikarya, and that CK1 might restrict neurofilament phosphorylation through activation of PP1.

The MAPK pathway, CDK5, CK1 and GSK3β each contribute to axonal neurofilament bunding

The above findings highlight that the activity of the MAPK pathway, CDK5, CK1 and GSK3β exert divergent roles on neurofilament dynamics, including inhibition of proteolysis (MAPK and CDK5; Fig. 5), restriction of neurofilament phosphorylation within perikarya, promotion of neurofilament transport into axonal neurites (MAPK and CK1; Figs 6,7) and promotion of bundling (CDK5, GSK3β; Figs 6,7). Given that the collective impact of these diverse functions would foster an increase in phospho-neurofilaments within axonal neurites, we considered that increased activity of each of these kinases would contribute either indirectly or directly to the establishment and maintenance of axonal neurofilament bundles. In support of this notion, overexpression of each of these kinases both increased the percentage of neurites displaying neurofilament bundles and CDK5, CK1 and GSK3β each increased the association of GFP–NF-H with bundles (Fig. 8A,B). These findings confirm that each of these kinases contributes directly or indirectly to the incorporation of neurofilaments into axonal bundles.

The distal portion of the NF-H C-terminal is essential for bundling

To address further the role of GSK3β in bundling, we compared incorporation into the bundle-enriched fraction of full-length GFP–NF-H with incorporation of GFP–NF-H in which the terminal 187 amino acids [the region of the C-terminal sidearm reported to be essential for bundling (Chen et al., 2000)] had been deleted (NF-HΔ187). Cells expressing HΔ187 generated prominent GFP-reactive species migrating at ~150 kDa on SDS gels, which corresponds to the anticipated migratory position of 115-kDa NF-H (i.e. lacking the terminal 187 amino

Journal of Cell Science (2014) 127, 4064–4077 doi:10.1242/jcs.153346

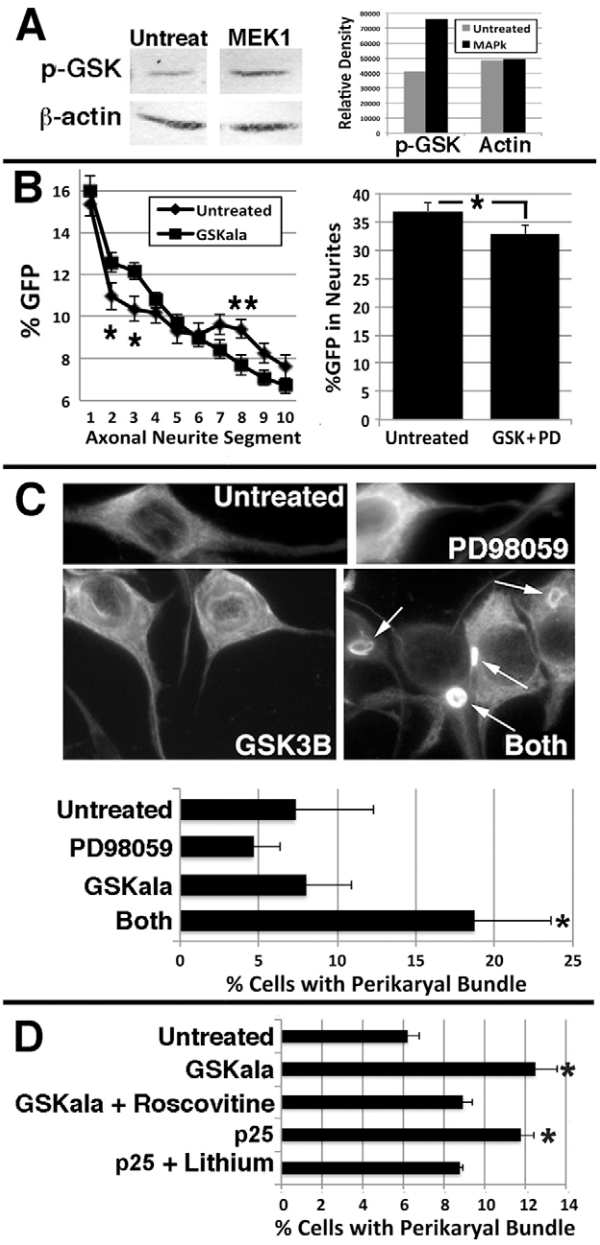

Fig. 6. GSK3β-mediated neurofilament–neurofilament associations require CDK5 and are inhibited by the MAPK pathway. (A) Nitrocellulose replicas of homogenates from cells with or without overexpression of MKK1 (MEK1), probed with an antibody directed against GSK3β phosphorylated at Ser9 (p-GSK), and homogenates expressing GFP–NF-H with or without PD98059 treatment and probed with RMO24. β-actin was used as loading control. The accompanying graph presents phospho-GSK3β and actin levels. Note overexpression of MKK1 increased phospho-GSK3β. (B) The left-most graph presents quantification of GFP–NF-H along axonal neurites ($n=19$ for each condition). *$P<0.05$ for the increase in GFP in segments of cells expressing GSKala versus untreated cells; **$P<0.05$ for the decrease in GFP in segments of cells expressing GSKala versus untreated cells. Values represent the mean±s.e.m. percentage GFP in each of the ten axonal segments. The right-most graph presents the percentage of total GFP with axonal neuritis. GSK3β overexpression plus PD98059 treatment significantly (*$P<0.05$) reduced overall GFP–NF-H levels. (C) Representative epifluorescence images of cells expressing GFP–NF-H with or without GSKala (GSK3B label) co-expression and PD98059 treatment. Note increased perikaryal and decreased neuritic GFP immunoreactivity following PD98059 treatment, and perikaryal neurofilament bundles (arrows) in PD98049-treated cells expressing GSKala. PD98059 + GSKala treatment increased the percentage of cells containing perikaryal neurofilament bundles (*$P<0.05$, ANOVA). $P<0.01$ for PD98059 + GSKala versus PD98059 alone; $P<0.06$ for PD98059 + GSKala versus untreated). Values represent the mean±s.e.m. percentage of cells ($n\geq20$ cells per condition). (D) Overexpression of GSKala or CDK5 increased perikaryal neurofilament bundles ($P<0.001$; ANOVA). Post hoc analyses with a Turkey–Kramer test for differences between means, and Fischer least significant difference (LSD) each revealed that perikaryal bundling in cells overexpressing GSKala and in cells overexpressing CDK5 differed from that in untreated cells (*$P<0.001$, for both tests). Roscovitine prevented the GSK3ala-mediated increase, whereas Li^+ prevented the CDK5-mediated increase; values for these conditions remained statistically identical to that of untreated cells (ANOVA with above post-hoc analyses). Values represent the mean±s.e.m. percentage of cells containing perikaryal neurofilament bundles.

acids) fused to GFP. Additional slower-migrating GFP-reactive species were observed between 155 and 175 kDa (Fig. 8C), and these displayed prominent immunoreactivity with antibodies directed against phospho-dependent neurofilament C-terminal epitopes (RT97, SMI34 and SMI31), confirming retention of these epitopes within the proximal portion of the sidearm. Retardation of migration of phospho-reactive HΔ187 isoforms demonstrates its ability to undergo phospho-mediated conformation alterations that foster retardation of full-length NF-H migration on SDS gels (Pant and Veeranna, 1995; Shea and Chan, 2008).

GFP–NF-HΔ187 co-assembled with the endogenous neurofilament network as shown by its distribution within the cytoskeleton and colocalization with filamentous profiles (Fig. 8D). Despite deletion of the portion of the NF-H sidearm purported to mediate neurofilament–neurofilament bundling, GFP–NF-HΔ187 was found within bundles both in cellular fractionation and immunofluorescence analyses (Fig. 5B,C), in a manner that was mediated by C-terminal crosslinking among endogenous (full-length) NF-H co-assembled into the same neurofilaments as shown previously (Kushkuley et al., 2009; Lee et al., 2011).

We next compared the influence of overexpression of GSK3β and CK1, because the majority of NF-H consensus sites for these kinases exist within the distal-most 187 amino acids (Chen et al., 2000; Hollander and Bennett, 1992; Hollander et al., 1996; Sasaki et al., 2002; Shaw et al., 1997), on bundling of GFP–NF-H and GFP–NF-HΔ187 (Fig. 8E). In the absence of kinase overexpression, both GFP–NF-H and GFP–NF-HΔ187 displayed an identical relative distribution within bundles versus the surrounding axoplasm. However, overexpression of GSK3β or CK1 each increased the relative amount of GFP–NF-H that was associated with axonal bundles, but did not alter the association of GFP–NF-HΔ187 within bundles. These findings suggest that GSK3β- and CK1-mediated phosphorylation of sites within the distal 187 amino acid residues of the NF-H C-terminal tail plays a crucial role in neurofilament bundling.

DISCUSSION

Key phosphorylation events foster the neurofilament–neurofilament associations that generate the stationary phase. Neurons are faced with the task of preventing or eliminating those events within perikarya, which would otherwise result in accumulation of perikaryal spheroids of phospho-neurofilaments, which are characteristic of conditions such as ALS, yet promoting these events within axons, without which the developing axon will

Journal of Cell Science (2014) 127, 4064–4077 doi:10.1242/jcs.153346

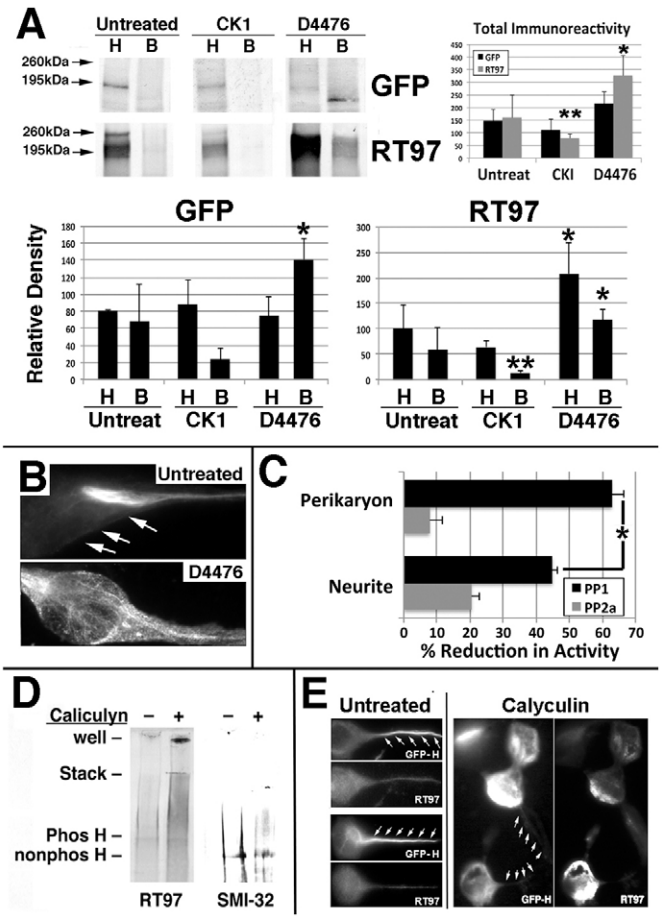

Fig. 7. CK1 inhibits neurofilament phosphorylation by activation of PP1. (A) Nitrocellulose replicas of total homogenates (H) and bundle fractions (B) from cells expressing GFP–NF-H with or without CK1 overexpression or D4476 treatment. The accompanying graphs present the total cellular immunoreactivity (and, separately, the amount within the H and B fractions, as indicated. Values represent the mean±s.d. $^{**}P<0.05$ for the decrease and $^{*}P<0.05$ for the increase in GFP–NF-H or RT97-reactive NF-H versus untreated cells (ANOVA with post-hoc analyses). (B) Representative image of RT97 immunoreactivity with and without D4476 treatment. Arrows denote the perikaryon. (C) D4476 reduced PP1 activity preferentially in soma ($^{*}P<0.01$; Student's *t* test) but not PP2A activity. (D) Immunoblot analyses of cells with or without calyculin treatment probed with RT97 and SMI-32. Calyculin induced formation of SDS-resistant aggregates of phospho-neurofilaments that were unable to penetrate the stacking gel (Stack). Phos H, phosphorylated NF-H; nonphos H, unphosphorylated NF-H. (E) Cells expressing GFP–NF-H (GFP-H) with or without calyculin treatment, probed with RT97. Note calyculin treatment induced the accumulation of phospho-neurofilaments within perikarya and reduced phospho-neurofilaments within neurites (arrowheads).

not undergo stabilization (Julien and Mushynski, 1998; Pant and Veeranna, 1995; Shea and Lee, 2011; Shea and Lee, 2013). The findings presented herein elucidate divergent roles for neurofilament kinases and phosphatases that encompass axonal transport and the establishment and/or maintenance of the stationary phase. These functions were mediated in part by direct phosphorylation of neurofilaments, but also by interactions among kinases and phosphatases.

We demonstrated herein that GSK3β activity is essential for neurofilament–neurofilament interactions leading to incorporation of neurofilaments into the stationary phase, which is readily seen in NB2a/d1 cells and cultured neurons by the appearance of tightly associated 'bundled' neurofilaments (Kushkuley et al., 2009; Yabe et al., 2001a; Yuan et al., 2009). However, GSK3β-induced bundling was not restricted to axonal neurites but also occurred within perikarya. We demonstrated herein that the MAPK pathway, activity of which is essential for transport of neurofilaments into and along axonal neurites of NB2a/d1 cells (Chan et al., 2004), promotes neurofilament axonal transport by inhibiting GSK3β activity: increasing MAPK pathway activity increased GSK3β phosphorylation at Ser9 [which inactivates GSK3β (Sutherland et al., 1993)] and prevented GSK3β-induced neurofilament–neurofilament association, whereas inhibition of MAPK pathway activity potentiated GSK3β-induced inhibition of axonal transport and accumulation of neurofilament bundles within perikarya.

CK1 activated PP1, which was essential for translocation of neurofilaments out of perikarya and into axonal neurites; inhibition of CK1 activity or direct inhibition of PP1 fostered accumulation of phospho-neurofilament immunoreactivity and neurofilament bundles within perikarya. This finding suggests that the normal segregation of extensive phosphorylation and resultant neurofilament bundling to axons is achieved by maintaining a relatively higher ratio of phosphatase to kinase activity within perikarya than within axonal neurites. This possibility is consistent with the rapid *de novo* accumulation of phospho-neurofilament immunoreactivity within retinal ganglion cell perikarya and proximal axons *in situ* following inhibition of PP2A (Jung and Shea, 1999).

The above findings demonstrate essential roles for the MAPK pathway and CK1 in promotion of neurofilament transport out of perikarya. We did not determine whether or not the MAPK pathway and CK1 mediated continued transport of neurofilaments along axonal neurites by their respective inhibition of GSK3β and activation of PP1. However, transporting neurofilaments enter and leave the stationary cytoskeleton (Kushkuley et al., 2009; Lewis and Nixon, 1988; Nixon and Logvinenko, 1986; Trivedi et al., 2007; Yabe et al., 2001a; Yuan et al., 2009). This finding, coupled with the finding that there are increased phospho-neurofilaments along axons following inhibition of PP1 and PP2A (herein and Shea et al., 1993), suggests that there are ongoing cycles of neurofilament phosphorylation and dephosphorylation within axons.

In addition to regulation of PP1 activity, CK1 mediated an NF-H migratory shift on SDS gels from 160 kDa to 200 kDa. Herein, we observed prominent RT97 immunoreactivity with the entire range of NF-H isoforms, including the 160-kDa isoform, following CK1 inhibition. This was unexpected, because RT97 immunoreactivity, which is generated by the MAPK pathway (Veeranna et al., 2008), is normally associated with the most highly phosphorylated NF-H isoforms, migrating at ≥200 kDa (Jung and Shea, 1999; Veeranna et al., 2008; Yabe et al., 2000). However, prior studies have not simultaneously manipulated CK1 along with proline-directed CDK5 and MAPK activity. Given that CK1 is constitutively active, CK1-mediated phosphorylation events responsible for the shift of NF-H from 160 to 200 kDa would occur constitutively and independently of MAPK activity; whereas MAPK manipulation alters RT97 immunoreactivity, this immunoreactivity would routinely be detected on isoforms already phosphorylated by CK1. This line of reasoning is supported by the observation of 200-kDa NF-H within perikarya and axonal hillocks, whereas RT97 is normally restricted to the axonal shaft (Jung and Shea, 1999; Sánchez et al., 2000; Yabe et al., 2000).

Journal of Cell Science (2014) 127, 4064–4077 doi:10.1242/jcs.153346

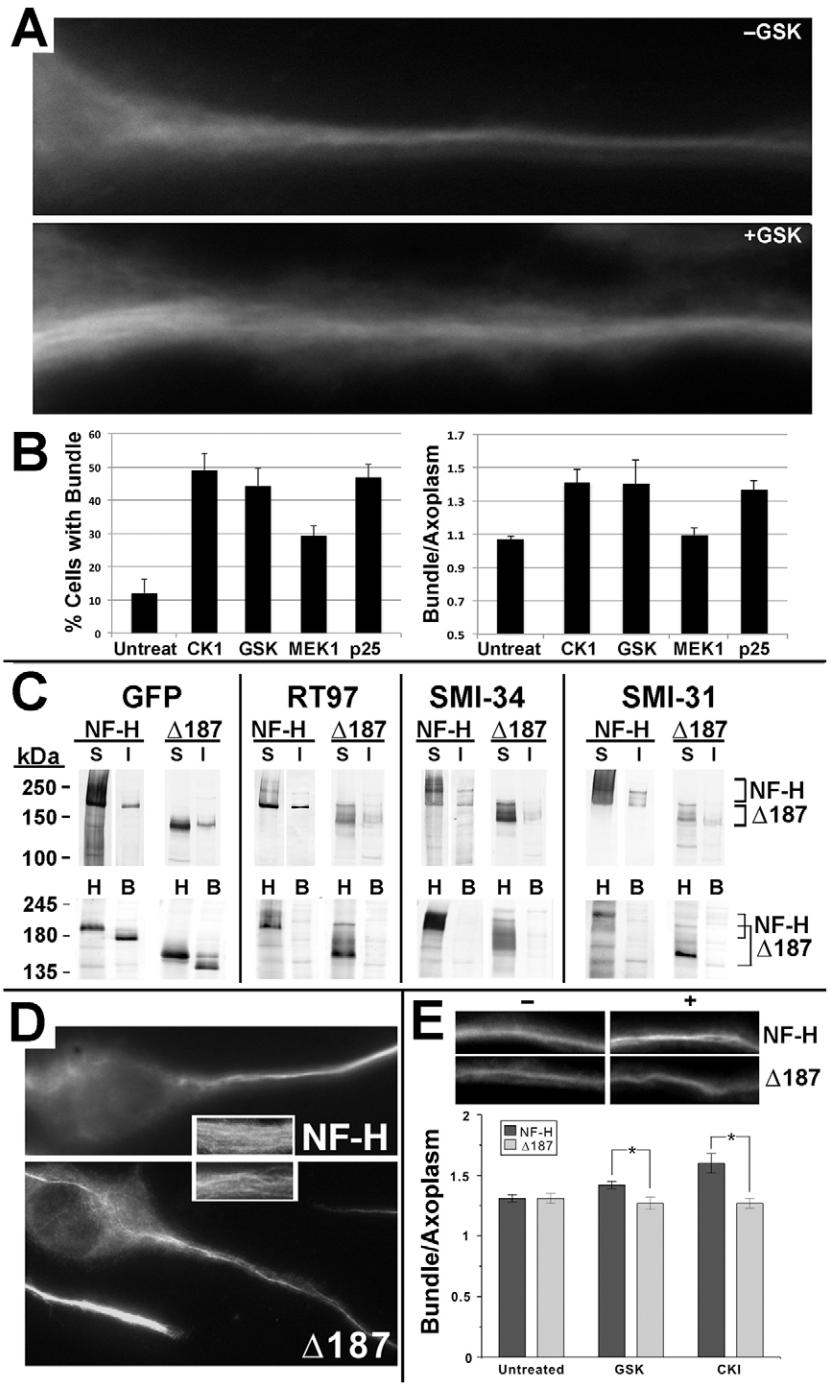

Fig. 8. Multiple neurofilament kinases contribute to neurofilament bundling. (A) Representative images of the hillock and axonal neurite of cells expressing GFP–NF-H with or without GSK3β overexpression. (B) The percentage of cells displaying GFP-labeled neurofilament bundles and the relative densitometric intensity of GFP within bundles versus the surrounding axoplasm for cells expressing GFP–NF-H with or without kinase overexpression (MEK1, MKK1). The percentage of cells with bundles was increased following overexpression of all kinases ($P<0.05$; ANOVA). The ratio of GFP in bundles versus axoplasm was increased ($P<0.05$) following overexpression of all kinases except MKK1. Values represent the mean±s.e.m. from multiple cells from duplicate experiments. (C) The upper row presents nitrocellulose replicas of Triton-soluble (S) and insoluble (I) fractions from cells expressing GFP–NF-H and GFP-NF-HΔ187 (Δ187) probed with RT97, SMI-34 and SMI-31. The lower row presents nitrocellulose replicas of initial homogenates (H) and bundle (B) fractions from cells expressing NF-H or NF-HΔ187. Migratory positions of each fusion protein are indicated along the right of each panel. Fractions from cells expressing GFP-tagged full-length NF-H displayed prominent GFP-reactive species migrating at ~195–250 kDa on SDS gels, corresponding to the migratory position of NF-H fused to 30–35-kDa GFP. Fractions from cells expressing NF-HΔ187 displayed a prominent 150-kDa GFP-reactive species, corresponding to the migratory position of the NF-H fragment fused to GFP; additional slower-migrating GFP-reactive species were observed between 155 and 175 kDa. Note NF-HΔ187 retained immunoreactivity with all antibodies and incorporated into the cytoskeleton and the bundle-enriched fraction, indicating co-assembly with endogenous neurofilaments. Minor additional immunoreactive species correspond to endogenous NF-H (160–205 kDa) and NF-M (125–140 kDa). (D) Representative cells overexpressing GFP–NF-H and NF-HΔ187, and immunostained with RT97. Note the distribution along axons, including their association with the centrally situated neurofilament bundle. Inserts: higher magnification of axonal neurites depicting filamentous profiles. (E) Representative images of the central region of axonal neurites of cells expressing GFP-tagged full-length NF-H or HΔ187, with (+) and without (–) overexpression of CK1 as indicated. The accompanying graph depicts the ratio of GFP intensity within bundle versus the surrounding axoplasm calculated as described in the Materials and Methods. This ratio was identical for NF-H and HΔ187 in the absence of kinase overexpression. GSK3β or CK1 overexpression increased this ratio for NF-H but not for NF-HΔ187. *$P<0.05$ (Student's *t* test).

The use of SDS gels containing a relatively low acrylamide content revealed an array of NF-H isoforms similar to those observed in optic pathway (Lewis and Nixon, 1988). Site-directed mutagenesis of CDK5-specific phosphorylation sites induced minor alterations in migration of NF-H migration on SDS gels. GSK3β activity induced RMO-24 reactivity and the appearance of the slowest-migrating neurofilament isoform, corresponding to the 210-kDa isoform in optic pathway (Lewis and Nixon, 1988). Inhibition of the MAPK pathway depleted this slowest-migrating isoform, indicating that a combination of MAPK and GSK3β activity generated this isoform.

Phosphorylation inhibits neurofilament proteolysis (Pant and Veeranna, 1995). Our findings have provided further insight into this regulation by demonstrating that phosphorylation by CDK5 and MAPK, and not by CK1 and/or GSK3β, mediated this protection. We observed increased NF-H proteolysis following simultaneous inhibition of CDK5 and the MAPK pathway but not upon inhibition of GSK3β or CK1, and overexpression of GSK3β and CK1 failed to prevent NF-H proteolysis following inhibition of CDK5 and the MAPK pathway. These findings indicate that phosphorylation of the KSP domains provides protection against proteolysis. Given that the terminal 187 amino acid residues, which contains the majority of the CK1 and GSK3β consensus sequences, is essential for bundling (Chen et al., 2000), one speculation arising from the differential impact of these kinases on proteolysis and bundling is that the C-terminal 187 amino acid

Journal of Cell Science (2014) 127, 4064–4077 doi:10.1242/jcs.153346

residues, rather than the KSP-rich regions, might mediate the cation-dependent crosslinking that incorporates neurofilaments into bundles (Kushkuley et al., 2009), leaving the more proximal KSP-rich region, or a portion of it, exposed to potential protease activity. If this were indeed the case, dephosphorylation of the KSP-rich region could allow proteolysis of bundled neurofilaments, which might provide a means for localized remodeling of the cytoskeleton, including any required axonal branching (Xie et al., 2006).

Comparison of GFP–NF-H within axonal neurites and bundles indicated that CK1, GSK3β and CDK5 all increased bundling of neurofilaments, indicating that once neurofilaments were within axons, all of these kinases contributed to the establishment and maintenance of the stationary phase. However, our systematic overexpression and inhibition highlighted that these kinases regulated a hierarchical series of events encompassing proteases and phosphatases. GSK3β-mediated neurofilament bundling required prior phosphorylation of those neurofilaments by CDK5. MAPK-pathway-mediated downregulation of GSK3β activity within perikarya was essential to restrict segregation of bundling within axonal neurites. Like the MAPK pathway, CK1 also promoted neurofilament transport into axonal neurites by restricting the accumulation of extensive phosphorylation within perikarya, although CK1 mediated this by activation of PP1 rather than inhibition of GSK3β. In addition, inhibition of neurofilament proteolysis by CDK5 and MAPK also likely contributed to bundling by maintaining sufficient concentration of axonal neurofilaments. Promotion of neurofilament transport into axons by the MAPK pathway and CK1, inhibition of neurofilament proteolysis by the MAPK pathway and CDK5, and prior neurofilament phosphorylation at least by CDK5 represent mechanisms by which these kinases could contribute to GSK3β-induced neurofilament bundling within axons. These findings collectively indicate that the impact on neurofilament dynamics of the non-proline-directed kinases CK1 and GSK3β are functionally regulated by the proline-directed neurofilament kinases of the MAPK pathway and CDK5.

A limitation of these analyses is that we did not dephosphorylate neurofilaments prior to examination of the impact of kinase manipulation. Accordingly, we cannot completely exclude the possibility that prior phosphorylation events contributed to the changes observed following manipulation of individual kinases. Unfortunately, experimental neurofilament dephosphorylation results in rapid proteolysis within cells (Pant and Veeranna, 1995) and under cell-free conditions because of neurofilament-associated proteases (Kushkuley et al., 2009). A further limitation is that we were unable to examine the consequences of simultaneous overexpression of multiple kinases. We have routinely manipulated kinases in cells co-transfected with GFP–NF-H or GFP–NF-M by utilizing two times more of the respective kinase construct versus the GFP-tagged neurofilament construct. To examine the consequence of multiple kinases would require successful triple transfection (i.e. GFP–NF-H plus two or more kinase constructs), which is impractical.

The kinases studied herein have multiple substrates beyond neurofilaments. As such, we cannot exclude the possibility that at least some of the impact of kinase and/or phosphatase manipulation on neurofilaments, as seen hererin, was derived by indirect effects on other cellular pathways. For example, although neurofilament phosphorylation clearly provides resistance to proteolysis (Pant and Veeranna, 1995), we cannot exclude the possibility that manipulation of kinase and/or phosphatase activities also suppressed activity of proteolytic enzymes themselves, which would further contribute to increased neurofilament levels. Similarly, whereas phosphorylation promotes neurofilament bundling, and in doing so removes neurofilaments from the transporting pool (Shea and Lee, 2011; Kushkuley et al., 2009), the kinases examined herein also directly and indirectly have an impact on kinesin itself (Morfini et al., 2002). We therefore cannot completely exclude the possibility that at least some of the alterations in neurofilament distribution following kinase and/or phosphatase manipulations were derived at least in part from disruptions in overall axonal transport. This likelihood is reduced, however, by our prior demonstration that manipulation of the MAPK pathway and CDK5 by the same methodologies utilized herein did not alter axonal transport of tau (which is also dependent upon kinesin) in these cells (Moran et al., 2005; Dubey et al., 2008). Notably, even if the kinases and phosphatases studied herein mediate some of their impact on neurofilaments by modulation of proteolytic and transport systems, it does not diminish the overall conclusion that the collective impact of these divergent kinase activities increases the amount of phospho-neurofilaments within axonal neurites, which in turn contributes to establishment and maintenance of the stationary phase.

C-terminal neurofilament phosphorylation does not directly interfere with neurofilament axonal transport, but indirectly interferes with transport by allowing some neurofilaments to withdraw from the transporting pool to establish the stationary cytoskeleton, which is essential for axonal maturation. This avoids the need for any alteration in the transport system itself to foster axonal maturation. Notably, this allows continued activity of transport systems within axons. Using the same transport battery throughout neuronal differentiation and maturation simplifies these dynamics, allows stabilization of proximal axonal regions while distal regions are still elongating, and ultimately allows transition into a maintenance system that can repair and replace damaged or worn out neurofilaments at any locus along the axon.

The kinases studied herein share pivotal roles in neuronal homeostasis. Any requirement to modulate their activity to foster neurofilament transport and assembly of the stationary phase would impact on multiple essential neuronal pathways. However, given that extensively phosphorylated neurofilaments essentially undergo self-assembly to form the stationary phase within axons, there is no apparent requirement for a developing neuron to modulate the activity of these kinases, nor their corresponding phosphatases, for establishment or repair of the stationary phase. Intermediate filaments provide mechanical strength to cells and mediate the formation of tissues (Fuchs, 1994). Perhaps nowhere can the need for long-term, stable structural support be more crucial than in axons, which, once synaptogenesis has occurred, remain in place for the lifetime of the individual (Shea and Lee, 2013). The interplay of kinase and phosphatase activities on neurofilament dynamics as demonstrated herein demonstrate how this class of intermediate filaments can establish a long-lasting and supportive macrostructure polarity during development without the need to alter activity of participating kinases or that of the overall transport system.

MATERIALS AND METHODS

Differentiation

Mouse NB2a/d1 neuroblastoma cells were cultured in DMEM containing 10% fetal bovine serum and differentiated with 1 mM dibutyryl cyclic

AMP (dbcAMP) (Yabe et al., 1999). For simplicity and clarity of writing, translocation of neurofilaments into and along axonal neurites of these cells is referred to as 'axonal transport'.

Expression of neurofilament constructs

Cells were transfected using Lipofectamine (Invitrogen, Carlsbad, CA) with constructs expressing GFP-tagged full-length NF-H (GFP–NF-H), the GFP-tagged isolated NF-H sidearm (i.e. lacking the rod domain, wild-type GFP–NF-H sidearms), GFP-tagged sidearms in which the serine residues in the C-terminal CDK5 consensus sites were mutated to aspartate residues (GFP–NF-Hasp) or alanine residues (GFP–NF-Hala) to mimic permanently phosphorylated or nonphosphorylated states (Ackerley et al., 2003; Lee et al., 2011), and GFP-tagged rat NF-H lacking the distal-most C-terminal 187 amino acids (GFP–NF-HΔ187). GFP–NF-HΔ187 was prepared from the above full-length GFP-tagged NF-H construct. Given that there is a unique AccI site in the C-terminal region of the rod domain of NF-H (Chen et al., 2000), the sequence between AccI and the last KSP motif was amplified by PCR using the following set of primers: 5′-AGAGTCGC-CAAAGTGAACACGGATGCT-3′ and 5′-CTGAGGATCCTAAGGGG-ACTTCACTTC-3′. Amplified PCR fragments were digested with AccI and BamHI, for which consensus sites were included in the primers, then cloned into the prepared template plasmid digested with the same enzymes. A ≥70% transfection efficiency for GFP-tagged neurofilament constructs is attained under these conditions (Chan et al., 2004).

Manipulation of kinase activities

Cells were transfected with a plasmid expressing constitutively active mouse GSK3β (a generous gift from Chris Miller, Institute of Psychiatry, King's College, UK), mouse CK1-α (denoted CK1 herein, Origene, Rockville, MD), constitutively active MKK1 (an upstream activator of the MAPK pathway) (Li et al., 1999) and p25 [the truncated and constitutively active form of the CDK5 activator p35 (Patrick et al., 1999)]. Additional cultures were treated with the pharmacological inhibitors roscovitine (20 μM), PD98059 (10 μM), Li^+ (10 mM), D4476 (100 μM) and tetrabromobenzotriazole (tBBT; 60 μM), which are active against CDK5, MKK1, GSK3β, CK1 and CK2 respectively (Cheng et al., 1983; Dudley et al., 1995; Meijer et al., 1997; Rena et al., 2004; Sarno et al., 2001). Given that the downstream impact of manipulation of MKK1 on neurofilaments is alteration of ERK1/2 kinases, we refer to MAPK pathway manipulation at points for simplicity of writing. For co-transfection with kinases and GFP–NF-H, more than two times of the kinase constructs versus GFP–NF-H were utilized (1 μg and 0.5 μg respectively); insuring that cells displaying GFP were co-transfected with the kinase construct (Chan et al., 2004; Shea et al., 2004).

Fractionation

Cells were homogenized in 50 mM Tris-HCl, pH 6.8, containing 1% Triton X-100, 5 mM EDTA, 1 mM PMSF and 50 μg/ml leupeptin and centrifuged (15,000 ***g***; 15 min). The resulting pellet was defined as the Triton-insoluble cytoskeleton, and the resulting supernatant was defined as the Triton-soluble fraction. Spinal cord neurofilaments from adult C57BL6 mice of both genders (all animal procedures were carried out in accordance with the approval of our Institutional Animal Care and Use Committee) were resuspended in 0.1M MES, pH 6.8, containing 1 mM $MgCl_2$, 1 mM EGTA, 1 mM PMSF and 50 μg/ml leupeptin and labeled with Rhodamine as described previously (Kushkuley et al., 2009; Wagner et al., 2003).

To obtain fractions enriched in bundled neurofilaments, additional homogenates were layered over the same buffer containing 1 M sucrose, and centrifuged at 15,000 ***g*** for 15 min. Bundled neurofilaments sedimented through the sucrose cushion; 'individual' neurofilaments (not contained within bundles) were recovered at the sucrose interface (Kushkuley et al., 2009; Yabe et al., 2001a). Protein concentration was determined by a BCA assay (Thermo scientific).

Cell-free neurofilament manipulations

Individual neurofilaments obtained as described above were incubated with or without purified kinases (Kushkuley et al., 2009) for 2 h at 37℃ with 0.1 μg/μl CDK5 and its activator p35, ERK1/2 and/or GSK3β (Upstate Biochemicals, Lake Placid, NY). The percentage of neurofilaments aligned with three or more than other neurofilaments were quantified by using fluorescence microscopy (Kushkuley et al., 2009). Closely aligned neurofilaments typically splay apart at their ends, facilitating detection of multiple neurofilaments (Kushkuley et al., 2009).

Electrophoresis and immunoblot analysis

Samples were normalized according to total protein, subjected to SDS gel electrophoresis and transferred onto nitrocellulose. The bundled fraction was solubilized with 8 M urea for electrophoresis. Membranes were blocked with 5% BSA and 5 mM sodium fluoride in Tris-buffered saline containing 0.1% Tween-20 for 1 h then incubated overnight at 4℃ with antibodies directed against GFP (1:1000, Invitrogen) and antibodies directed against neurofilament phospho-epitopes [RT97 (generous gift of Brian Anderton, Institute of Psychiatry, London, UK), SMI-34 and SMI-31 (Covance; Dedham, MA) and RMO-24 (Invitrogen)], nonphospho-epitopes (SMI-32) and an antibody directed against neurofilaments regardless of phosphorylation state (R39) (Jung and Shea, 1999). Membranes were washed with the same buffer then incubated with alkaline-phosphatase-conjugated secondary antibodies for 1 h at room temperature and developed using a NBT/BCIP substrate kit (Promega, Madison, WI). Immunoreactive species were quantified in digitized images of replicas using Image J; the background signal from an adjacent, identically sized, area in the identical lane was subtracted from each reactive species (Yabe et al., 2001a; Yabe et al., 1999). All samples to be compared were electrophoresed on the same gel, transferred onto nitrocellulose and visualized simultaneously.

Immunofluorescence

Cells grown on poly-L-Lysine-treated coverslips were fixed with 4% paraformaldehyde in phosphate-buffered saline (PBS, pH 7.4) for 10 min at room temperature, rinsed two times in PBS (5 min/rinse), and blocked for 30 min in PBS containing 1% BSA and 2% normal goat serum. Cultures were then incubated overnight at 4℃ in PBS containing 1% BSA and a 1:500 dilution of anti-GFP antibody or against R39, or 1:100 dilutions of antibodies against RT97, SMI34, SMI-31, SMI-32 and RMO-24. Cultures were rinsed three times with PBS, incubated for 30 min at 37℃ in PBS containing 1% BSA and 1:300 dilutions of appropriate secondary antibodies.

Monitoring of intracellular neurofilament distribution

Neurofilament distribution was quantified using ImageJ. Translocation of neurofilament constructs into and along axonal neurites was quantified as an index of axonal transport. The shaft of axonal neurites was divided into ten equivalent segments, excluding the hillock and the growth cone, and the percentage of GFP within each segment was calculated relative to the total GFP within the axonal shaft (Yabe et al., 2001b). In additional studies, axonal neurites (>25 for each condition) were divided into three equivalent segments (defined as proximal, central and distal), excluding the hillock and growth cone. The translocation rate was determined by dividing the GFP intensity in the distal fragment by that of central fragment within each neurite (Chan et al., 2004). To monitor the extent of incorporation of GFP-tagged neurofilaments into axonal neurofilament bundles, the GFP intensity of the bundle and that of the area adjacent to the bundle were quantified within the central neurite segment for >20 cells for each condition (Chan et al., 2004; Chan et al., 2005).

Kinase and phosphatase assays

GSK3β activity was assayed by monitoring phosphorylation of GSK3β at Ser9 (which inactivates GSK3β) and phosphorylation of the GSK3β substrate β-catenin at Ser33, Ser37 and Thr41. Homogenates of cells with or without GSK3β overexpression or 10 mM Li^+ treatment were subjected to electrophoresis, transferred onto nitrocellulose and probed with antibodies directed against total GSK3β, GSK3β that had been phosphorylated at Ser9, total β-catenin, and β-catenin phosphorylated at Ser33, Ser37 and Thr41 (Cell Signaling), and, as a loading control, anti-tubulin antibody DM1A. Given that β-catenin is degraded once

phosphorylated by GSK3β (Ding et al., 2005), a decrease in phospho-β-catenin (which can also be reflected in total β-catenin levels) provides an index of GSK3β activity.

CK1 activity was monitored by casein gel zymology (Cheng and Louis, 1999). Lysates from cells incubated for 4 h with or without 100 µM D4476 were separated on a 12% polyacrylamide gel polymerized in the presence of 1 mg/ml dephosphorylated casein. After electrophoresis, SDS was removed from the gel by rinsing twice for 30 min with 50 mM Tris-HCl, pH 8.0, containing 20% isopropanol. The gel was washed twice for 30 min in 50 mM Tris-HCl containing 5 mM 2-mercaptoethanol. Electrophoresed proteins were denatured by incubating the gel twice for 30 min in the above buffer containing 6 M guanidine-HCl, and were then renatured by 15 h of washing at 4℃ in four changes of the above buffer containing 0.05% Tween 40. The gel was equilibrated in 10 mM Tris-HCl, pH 7.5, containing 10 mM $MgCl_2$ for 30 min at room temperature. Casein phosphorylation was carried out by incubation of the gel in 10 mM Tris-HCl, pH 7.5, containing 10 mM $MgCl_2$, 25 µM ATP and 2.5 µCi/ml, [γ-^{32}P]ATP for 2 h at room temperature followed by washing with 5% trichloroacetic acid and 1% sodium pyrophosphate until no radioactivity was detected in the wash. The gel was dried and exposed to X-ray film.

Competing interests

The authors declare no competing interests.

Author contributions

S.L. performed all experiments. S.L. and T.B.S. prepared the final figures. S.L., H.P. and T.B.S. designed the experiments and wrote the manuscript.

Funding

This work was supported by the National Science Federation.

References

Ackerley, S., Grierson, A. J., Brownlees, J., Thornhill, P., Anderton, B. H., Leigh, P. N., Shaw, C. E. and Miller, C. C. (2000). Glutamate slows axonal transport of neurofilaments in transfected neurons. *J. Cell Biol.* **150**, 165-176.

Ackerley, S., Thornhill, P., Grierson, A. J., Brownlees, J., Anderton, B. H., Leigh, P. N., Shaw, C. E. and Miller, C. C. (2003). Neurofilament heavy chain side arm phosphorylation regulates axonal transport of neurofilaments. *J. Cell Biol.* **161**, 489-495.

Adams, D. G., Coffee, R. L., Jr, Zhang, H., Pelech, S., Strack, S. and Wadzinski, B. E. (2005). Positive regulation of Raf1-MEK1/2-ERK1/2 signaling by protein serine/threonine phosphatase 2A holoenzymes. *J. Biol. Chem.* **280**, 42644-42654.

Bajaj, N. P. and Miller, C. C. (1997). Phosphorylation of neurofilament heavy-chain side-arm fragments by cyclin-dependent kinase-5 and glycogen synthase kinase-3alpha in transfected cells. *J. Neurochem.* **69**, 737-743.

Bajaj, N. P., al-Sarraj, S. T., Leigh, P. N., Anderson, V. and Miller, C. C. (1999). Cyclin dependent kinase-5 (CDK-5) phosphorylates neurofilament heavy (NF-H) chain to generate epitopes for antibodies that label neurofilament accumulations in amyotrophic lateral sclerosis (ALS) and is present in affected motor neurones in ALS. *Prog. Neuropsychopharmacol. Biol. Psychiatry* **23**, 833-850.

Barry, D. M., Millecamps, S., Julien, J. P. and Garcia, M. L. (2007). New movements in neurofilament transport, turnover and disease. *Exp. Cell Res.* **313**, 2110-2120.

Chan, W. K., Dickerson, A., Ortiz, D., Pimenta, A. F., Moran, C. M., Motil, J., Snyder, S. J., Malik, K., Pant, H. C. and Shea, T. B. (2004). Mitogen-activated protein kinase regulates neurofilament axonal transport. *J. Cell Sci.* **117**, 4629-4642.

Chan, W. K., Yabe, J. T., Pimenta, A. F., Ortiz, D. and Shea, T. B. (2005). Neurofilaments can undergo axonal transport and cytoskeletal incorporation in a discontinuous manner. *Cell Motil. Cytoskeleton* **62**, 166-179.

Chen, J., Nakata, T., Zhang, Z. and Hirokawa, N. (2000). The C-terminal tail domain of neurofilament protein-H (NF-H) forms the crossbridges and regulates neurofilament bundle formation. *J. Cell Sci.* **113**, 3861-3869.

Cheng, H. L. and Louis, C. F. (1999). Endogenous casein kinase I catalyzes the phosphorylation of the lens fiber cell connexin49. *Eur. J. Biochem.* **263**, 276-286.

Cheng, K., Creacy, S. and Larner, J. (1983). 'Insulin-like' effects of lithium ion on isolated rat adipocytes. II. Specific activation of glycogen synthase. *Mol. Cell. Biochem.* **56**, 183-189.

DeFuria, J. and Shea, T. B. (2007). Arsenic inhibits neurofilament transport and induces perikaryal accumulation of phosphorylated neurofilaments: roles of JNK and GSK-3beta. *Brain Res.* **1181**, 74-82.

Ding, Q., Xia, W., Liu, J. C., Yang, J. Y., Lee, D. F., Xia, J., Bartholomeusz, G., Li, Y., Pan, Y., Li, Z. et al. (2005). Erk associates with and primes GSK-3beta for its inactivation resulting in upregulation of beta-catenin. *Mol. Cell* **19**, 159-170.

Dubey, M., Chaudhury, P., Kabiru, H. and Shea, T. B. (2008). Tau inhibits anterograde axonal transport and perturbs stability in growing axonal neurites in part by displacing kinesin cargo: neurofilaments attenuate tau-mediated neurite instability. *Cell Motil. Cytoskeleton* **65**, 89-99.

Dudley, D. T., Pang, L., Decker, S. J., Bridges, A. J. and Saltiel, A. R. (1995). A synthetic inhibitor of the mitogen-activated protein kinase cascade. *Proc. Natl. Acad. Sci. USA* **92**, 7686-7689.

Fuchs, E. (1994). Intermediate filaments and disease: mutations that cripple cell strength. *J. Cell Biol.* **125**, 511-516.

Galletti, M., Riccardo, S., Parisi, F., Lora, C., Saqcena, M. K., Rivas, L., Wong, B., Serra, A., Serras, F., Grifoni, D. et al. (2009). Identification of domains responsible for ubiquitin-dependent degradation of dMyc by glycogen synthase kinase 3beta and casein kinase 1 kinases. *Mol. Cell. Biol.* **29**, 3424-3434.

Giasson, B. I. and Mushynski, W. E. (1997). Study of proline-directed protein kinases involved in phosphorylation of the heavy neurofilament subunit. *J. Neurosci.* **17**, 9466-9472.

Goldberg, Y. (1999). Protein phosphatase 2A: who shall regulate the regulator? *Biochem. Pharmacol.* **57**, 321-328.

Gong, C. X., Wang, J. Z., Iqbal, K. and Grundke-Iqbal, I. (2003). Inhibition of protein phosphatase 2A induces phosphorylation and accumulation of neurofilaments in metabolically active rat brain slices. *Neurosci. Lett.* **340**, 107-110.

Grant, P., Sharma, P. and Pant, H. C. (2001). Cyclin-dependent protein kinase 5 (Cdk5) and the regulation of neurofilament metabolism. *Eur. J. Biochem.* **268**, 1534-1546.

Guan, R. J., Khatra, B. S. and Cohlberg, J. A. (1991). Phosphorylation of bovine neurofilament proteins by protein kinase FA (glycogen synthase kinase 3). *J. Biol. Chem.* **266**, 8262-8267.

Guidato, S., Tsai, L. H., Woodgett, J. and Miller, C. C. (1996). Differential cellular phosphorylation of neurofilament heavy side-arms by glycogen synthase kinase-3 and cyclin-dependent kinase-5. *J. Neurochem.* **66**, 1698-1706.

Hagen, T., Di Daniel, E., Culbert, A. A. and Reith, A. D. (2002). Expression and characterization of GSK-3 mutants and their effect on beta-catenin phosphorylation in intact cells. *J. Biol. Chem.* **277**, 23330-23335.

Harwood, A. J. (2002). Signal transduction in development: holding the key. *Dev. Cell* **2**, 384-385.

Henry, S. P. and Killilea, S. D. (1993). Hierarchical regulation by casein kinases I and II of the activation of protein phosphatase-1i by glycogen synthase kinase-3 is ionic strength dependent. *Arch. Biochem. Biophys.* **301**, 53-57.

Hergovich, A., Lisztwan, J., Thoma, C. R., Wirbelauer, C., Barry, R. E. and Krek, W. (2006). Priming-dependent phosphorylation and regulation of the tumor suppressor pVHL by glycogen synthase kinase 3. *Mol. Cell. Biol.* **26**, 5784-5796.

Hollander, B. A. and Bennett, G. S. (1992). Characterization of a neurofilament-associated kinase that phosphorylates the middle molecular mass component of chicken neurofilaments. *Brain Res.* **599**, 237-245.

Hollander, B. A., Bennett, G. S. and Shaw, G. (1996). Localization of sites in the tail domain of the middle molecular mass neurofilament subunit phosphorylated by a neurofilament-associated kinase and by casein kinase I. *J. Neurochem.* **66**, 412-420.

Holmgren, A., Bouhy, D. and Timmerman, V. (2012). Neurofilament phosphorylation and their proline-directed kinases in health and disease. *J. Peripher. Nerv. Syst.* **17**, 365-376.

Julien, J. P. and Mushynski, W. E. (1998). Neurofilaments in health and disease. *Prog. Nucleic Acid Res. Mol. Biol.* **61**, 1-23.

Jung, C. and Shea, T. B. (1999). Regulation of neurofilament axonal transport by phosphorylation in optic axons in situ. *Cell Motil. Cytoskeleton* **42**, 230-240.

Kesavapany, S., Li, B. S. and Pant, H. C. (2003). Cyclin-dependent kinase 5 in neurofilament function and regulation. *Neurosignals* **12**, 252-264.

Kushkuley, J., Chan, W. K., Lee, S., Eyer, J., Leterrier, J. F., Letournel, F. and Shea, T. B. (2009). Neurofilament cross-bridging competes with kinesin-dependent association of neurofilaments with microtubules. *J. Cell Sci.* **122**, 3579-3586.

Lamarre, M. and Desrosiers, R. R. (2008). Up-regulation of protein L-isoaspartyl methyltransferase expression by lithium is mediated by glycogen synthase kinase-3 inactivation and beta-catenin stabilization. *Neuropharmacology* **55**, 669-676.

Lee, S., Sunil, N. and Shea, T. B. (2011). C-terminal neurofilament phosphorylation fosters neurofilament-neurofilament associations that compete with axonal transport. *Cytoskeleton* **68**, 8-17.

Lewis, S. E. and Nixon, R. A. (1988). Multiple phosphorylated variants of the high molecular mass subunit of neurofilaments in axons of retinal cell neurons: characterization and evidence for their differential association with stationary and moving neurofilaments. *J. Cell Biol.* **107**, 2689-2701.

Li, B. S., Veeranna, Gu, J., Grant, P. and Pant, H. C. (1999). Activation of mitogen-activated protein kinases (Erk1 and Erk2) cascade results in phosphorylation of NF-M tail domains in transfected NIH 3T3 cells. *Eur. J. Biochem.* **262**, 211-217.

Link, W. T., Grant, P., Hidaka, H. and Pant, H. C. (1992). Casein kinases I and II from squid brain exhibit selective neurofilament phosphorylation. *Mol. Cell. Neurosci.* **3**, 548-558.

Liu, F., Ma, X. H., Ule, J., Bibb, J. A., Nishi, A., DeMaggio, A. J., Yan, Z., Nairn, A. C. and Greengard, P. (2001). Regulation of cyclin-dependent kinase 5 and casein kinase 1 by metabotropic glutamate receptors. *Proc. Natl. Acad. Sci. USA* **98**, 11062-11068.

Maccioni, R. B., Otth, C., Concha, I. I. and Muñoz, J. P. (2001). The protein kinase Cdk5. Structural aspects, roles in neurogenesis and involvement in Alzheimer's pathology. *Eur. J. Biochem.* **268**, 1518-1527.

Marston, F. A. and Hartley, D. L. (1990). Solubilization of protein aggregates. *Methods Enzymol.* **182**, 264-276.
Meijer, L., Borgne, A., Mulner, O., Chong, J. P., Blow, J. J., Inagaki, N., Inagaki, M., Delcros, J. G. and Moulinoux, J. P. (1997). Biochemical and cellular effects of roscovitine, a potent and selective inhibitor of the cyclin-dependent kinases cdc2, cdk2 and cdk5. *Eur. J. Biochem.* **243**, 527-536.
Moran, C. M., Donnelly, M., Ortiz, D., Pant, H. C., Mandelkow, E. M. and Shea, T. B. (2005). Cdk5 inhibits anterograde axonal transport of neurofilaments but not that of tau by inhibition of mitogen-activated protein kinase activity. *Brain Res. Mol. Brain Res.* **134**, 338-344.
Morfini, G., Szebenyi, G., Elluru, R., Ratner, N. and Brady, S. T. (2002). Glycogen synthase kinase 3 phosphorylates kinesin light chains and negatively regulates kinesin-based motility. *EMBO J.* **21**, 281-293.
Nixon, R. A. (1998). The slow axonal transport debate. *Trends Cell Biol.* **8**, 100.
Nixon, R. A. and Logvinenko, K. B. (1986). Multiple fates of newly synthesized neurofilament proteins: evidence for a stationary neurofilament network distributed nonuniformly along axons of retinal ganglion cell neurons. *J. Cell Biol.* **102**, 647-659.
Nixon, R. A. and Shea, T. B. (1992). Dynamics of neuronal intermediate filaments: a developmental perspective. *Cell Motil. Cytoskeleton* **22**, 81-91.
Noh, K. T., Son, K. H., Jung, I. D., Kang, H. K., Hwang, S. A., Lee, W. S., You, J. C. and Park, Y. M. (2012). Protein kinase C δ (PKCδ)-extracellular signal-regulated kinase 1/2 (ERK1/2) signaling cascade regulates glycogen synthase kinase-3 (GSK-3) inhibition-mediated interleukin-10 (IL-10) expression in lipopolysaccharide (LPS)-induced endotoxemia. *J. Biol. Chem.* **287**, 14226-14233.
Pan, Y. W., Storm, D. R. and Xia, Z. (2013). Role of adult neurogenesis in hippocampus-dependent memory, contextual fear extinction and remote contextual memory: new insights from ERK5 MAP kinase. *Neurobiol. Learn. Mem.* **105**, 81-92.
Pant, H. C. and Veeranna, (1995). Neurofilament phosphorylation. *Biochem. Cell Biol.* **73**, 575-592.
Patrick, G. N., Zukerberg, L., Nikolic, M., de la Monte, S., Dikkes, P. and Tsai, L. H. (1999). Conversion of p35 to p25 deregulates Cdk5 activity and promotes neurodegeneration. *Nature* **402**, 615-622.
Perrot, R., Berges, R., Bocquet, A. and Eyer, J. (2008). Review of the multiple aspects of neurofilament functions, and their possible contribution to neurodegeneration. *Mol. Neurobiol.* **38**, 27-65.
Pucilowska, J., Puzerey, P. A., Karlo, J. C., Galán, R. F. and Landreth, G. E. (2012). Disrupted ERK signaling during cortical development leads to abnormal progenitor proliferation, neuronal and network excitability and behavior, modeling human neuro-cardio-facial-cutaneous and related syndromes. *J. Neurosci.* **32**, 8663-8677.
Rao, M. V., Yuan, A., Campbell, J., Kumar, A. and Nixon, R. A. (2012). The C-terminal domains of NF-H and NF-M subunits maintain axonal neurofilament content by blocking turnover of the stationary neurofilament network. *PLoS ONE* **7**, e44320.
Rena, G., Bain, J., Elliott, M. and Cohen, P. (2004). D4476, a cell-permeant inhibitor of CK1, suppresses the site-specific phosphorylation and nuclear exclusion of FOXO1a. *EMBO Rep.* **5**, 60-65.
Saito, T., Shima, H., Osawa, Y., Nagao, M., Hemmings, B. A., Kishimoto, T. and Hisanaga, S. (1995). Neurofilament-associated protein phosphatase 2A: its possible role in preserving neurofilaments in filamentous states. *Biochemistry* **34**, 7376-7384.
Sánchez, I., Hassinger, L., Sihag, R. K., Cleveland, D. W., Mohan, P. and Nixon, R. A. (2000). Local control of neurofilament accumulation during radial growth of myelinating axons in vivo. Selective role of site-specific phosphorylation. *J. Cell Biol.* **151**, 1013-1024.
Sarno, S., Reddy, H., Meggio, F., Ruzzene, M., Davies, S. P., Donella-Deana, A., Shugar, D. and Pinna, L. A. (2001). Selectivity of 4,5,6,7-tetrabromobenzotriazole, an ATP site-directed inhibitor of protein kinase CK2 ('casein kinase-2'). *FEBS Lett.* **496**, 44-48.
Sasaki, T., Taoka, M., Ishiguro, K., Uchida, A., Saito, T., Isobe, T. and Hisanaga, S. (2002). In vivo and in vitro phosphorylation at Ser-493 in the glutamate (E)-segment of neurofilament-H subunit by glycogen synthase kinase 3beta. *J. Biol. Chem.* **277**, 36032-36039.
Shaw, G., Miller, R., Wang, D. S., Tang, D., Hollander, B. A. and Bennett, G. S. (1997). Characterization of additional casein kinase I sites in the C-terminal ''tail'' region of chicken and rat neurofilament-M. *J. Neurochem.* **69**, 1729-1737.
Shea, T. B. and Chan, W. K. (2008). Regulation of neurofilament dynamics by phosphorylation. *Eur. J. Neurosci.* **27**, 1893-1901.
Shea, T. B. and Lee, S. (2011). Neurofilament phosphorylation regulates axonal transport by an indirect mechanism: a merging of opposing hypotheses. *Cytoskeleton* **68**, 589-595.
Shea, T. B. and Lee, S. (2013). The discontinuous nature of neurofilament transport accommodates both establishment and repair of the axonal neurofilament array. *Cytoskeleton* **70**, 67-73.
Shea, T. B., Paskevich, P. A. and Beermann, M. L. (1993). The protein phosphatase inhibitor okadaic acid increases axonal neurofilaments and neurite caliber, and decreases axonal microtubules in NB2a/d1 cells. *J. Neurosci. Res.* **35**, 507-521.
Shea, T. B., Yabe, J. T., Ortiz, D., Pimenta, A., Loomis, P., Goldman, R. D., Amin, N. and Pant, H. C. (2004). Cdk5 regulates axonal transport and phosphorylation of neurofilaments in cultured neurons. *J. Cell Sci.* **117**, 933-941.
Shukla, V., Skuntz, S. and Pant, H. C. (2012). Deregulated Cdk5 activity is involved in inducing Alzheimer's disease. *Arch. Med. Res.* **43**, 655-662.
Sihag, R. K., Inagaki, M., Yamaguchi, T., Shea, T. B. and Pant, H. C. (2007). Role of phosphorylation on the structural dynamics and function of types III and IV intermediate filaments. *Exp. Cell Res.* **313**, 2098-2109.
Strack, S., Westphal, R. S., Colbran, R. J., Ebner, F. F. and Wadzinski, B. E. (1997). Protein serine/threonine phosphatase 1 and 2A associate with and dephosphorylate neurofilaments. *Brain Res. Mol. Brain Res.* **49**, 15-28.
Sutherland, C., Leighton, I. A. and Cohen, P. (1993). Inactivation of glycogen synthase kinase-3 beta by phosphorylation: new kinase connections in insulin and growth-factor signalling. *Biochem. J.* **296**, 15-19.
Trivedi, N., Jung, P. and Brown, A. (2007). Neurofilaments switch between distinct mobile and stationary states during their transport along axons. *J. Neurosci.* **27**, 507-516.
Veeranna, A., Amin, N. D., Ahn, N. G., Jaffe, H., Winters, C. A., Grant, P. and Pant, H. C. (1998). Mitogen-activated protein kinases (Erk1,2) phosphorylate Lys-Ser-Pro (KSP) repeats in neurofilament proteins NF-H and NF-M. *J. Neurosci.* **18**, 4008-4021.
Veeranna, L., Lee, J. H., Pareek, T. K., Jaffee, H., Boland, B., Vinod, K. Y., Amin, N., Kulkarni, A. B., Pant, H. C. and Nixon, R. A. (2008). Neurofilament tail phosphorylation: identity of the RT-97 phosphoepitope and regulation in neurons by cross-talk among proline-directed kinases. *J. Neurochem.* **107**, 35-49.
Veeranna, Y., Yang, D. S., Lee, J. H., Vinod, K. Y., Stavrides, P., Amin, N. D., Pant, H. C. and Nixon, R. A. (2011). Declining phosphatases underlie aging-related hyperphosphorylation of neurofilaments. *Neurobiol. Aging* **32**, 2016-2029.
Waetzig, V. and Herdegen, T. (2003). The concerted signaling of ERK1/2 and JNKs is essential for PC12 cell neuritogenesis and converges at the level of target proteins. *Mol. Cell. Neurosci.* **24**, 238-249.
Wagner, U., Utton, M., Gallo, J. M. and Miller, C. C. (1996). Cellular phosphorylation of tau by GSK-3 beta influences tau binding to microtubules and microtubule organisation. *J. Cell Sci.* **109**, 1537-1543.
Wagner, O. I., Lifshitz, J., Janmey, P. A., Linden, M., McIntosh, T. K. and Leterrier, J. F. (2003). Mechanisms of mitochondria-neurofilament interactions. *J. Neurosci.* **23**, 9046-9058.
Wang, J., Wang, X., Liu, R., Wang, Q., Grundke-Iqbal, I. and Iqbal, K. (2002). In vitro analysis of tau phosphorylation sites and its biological activity. *Chin. Med. Sci. J.* **17**, 13-16.
Xie, Z., Samuels, B. A. and Tsai, L. H. (2006). Cyclin-dependent kinase 5 permits efficient cytoskeletal remodelin – a hypothesis on neuronal migration. *Cereb. Cortex* **16 Suppl. 1**, i64-i68.
Yabe, J. T., Pimenta, A. and Shea, T. B. (1999). Kinesin-mediated transport of neurofilament protein oligomers in growing axons. *J. Cell Sci.* **112**, 3799-3814.
Yabe, J. T., Jung, C., Chan, W. K. and Shea, T. B. (2000). Phospho-dependent association of neurofilament proteins with kinesin in situ. *Cell Motil. Cytoskeleton* **45**, 249-262.
Yabe, J. T., Chylinski, T., Wang, F. S., Pimenta, A., Kattar, S. D., Linsley, M. D., Chan, W. K. and Shea, T. B. (2001a). Neurofilaments consist of distinct populations that can be distinguished by C-terminal phosphorylation, bundling, and axonal transport rate in growing axonal neurites. *J. Neurosci.* **21**, 2195-2205.
Yabe, J. T., Wang, F. S., Chylinski, T., Katchmar, T. and Shea, T. B. (2001b). Selective accumulation of the high molecular weight neurofilament subunit within the distal region of growing axonal neurites. *Cell Motil. Cytoskeleton* **50**, 1-12.
Yuan, A., Nixon, R. A. and Rao, M. V. (2006). Deleting the phosphorylated tail domain of the neurofilament heavy subunit does not alter neurofilament transport rate in vivo. *Neurosci. Lett.* **393**, 264-268.
Yuan, A., Sasaki, T., Rao, M. V., Kumar, A., Kanumuri, V., Dunlop, D. S., Liem, R. K. and Nixon, R. A. (2009). Neurofilaments form a highly stable stationary cytoskeleton after reaching a critical level in axons. *J. Neurosci.* **29**, 11316-11329.
Yuan, A., Rao, M. V., Veeranna, and Nixon, R. A. (2012). Neurofilaments at a glance. *J. Cell Sci.* **125**, 3257-3263.
Zheng, Y. L., Li, B. S., Kanungo, J., Kesavapany, S., Amin, N., Grant, P. and Pant, H. C. (2007). Cdk5 Modulation of mitogen-activated protein kinase signaling regulates neuronal survival. *Mol. Biol. Cell* **18**, 404-413.